



3 4456 0380471 0

# ornl

ORNL/TM-12630

**OAK RIDGE  
NATIONAL  
LABORATORY**

**MARTIN MARIETTA**

## Performance Analysis of Reciprocating Regenerative Magnetic Heat Pumping

### Final Report

D. T. Chen  
R. W. Murphy  
V. C. Mei  
F. C. Chen  
J. W. Lue  
M. S. Lubell

OAK RIDGE NATIONAL LABORATORY  
CENTRAL RESEARCH LIBRARY  
CIRCULATION SECTION  
4800N ROOM 173  
**LIBRARY LOAN COPY**  
DO NOT TRANSFER TO ANOTHER PERSON  
If you wish someone else to see this  
report, send in name with report and  
the library will arrange a loan.  
UCR-289 (1-77)

MANAGED BY  
MARTIN MARIETTA ENERGY SYSTEMS, INC.  
FOR THE UNITED STATES  
DEPARTMENT OF ENERGY

This report has been reproduced directly from the best available copy.

Available to DOE and DOE contractors from the Office of Scientific and Technical Information, P.O. Box 62, Oak Ridge, TN 37831; prices available from (615) 576-8401, FTS 626-8401.

Available to the public from the National Technical Information Service, U.S. Department of Commerce, 5285 Port Royal Rd., Springfield, VA 22161.

This report was prepared as an account of work sponsored by an agency of the United States Government. Neither the United States Government nor any agency thereof, nor any of their employees, makes any warranty, express or implied, or assumes any legal liability or responsibility for the accuracy, completeness, or usefulness of any information, apparatus, product, or process disclosed, or represents that its use would not infringe privately owned rights. Reference herein to any specific commercial product, process, or service by trade name, trademark, manufacturer, or otherwise, does not necessarily constitute or imply its endorsement, recommendation, or favoring by the United States Government or any agency thereof. The views and opinions of authors expressed herein do not necessarily state or reflect those of the United States Government or any agency thereof.

ORNL/TM-12630

310  
958

**PERFORMANCE ANALYSIS OF  
RECIPROCATING REGENERATIVE MAGNETIC HEAT PUMPING**

Final Report

D. T. Chen,<sup>#</sup> R. W. Murphy,<sup>\*</sup> V. C. Mei,<sup>\*</sup> F. C. Chen,<sup>\*</sup>  
J. W. Lue,<sup>+</sup> and M. S. Lubell<sup>+</sup>

Date Published: February 1994

Prepared for  
THERMAL SCIENCES RESEARCH PROGRAM  
ADVANCED INDUSTRIAL CONCEPTS DIVISION  
OFFICE OF INDUSTRIAL TECHNOLOGIES

Prepared by the  
OAK RIDGE NATIONAL LABORATORY  
managed by  
MARTIN MARIETTA ENERGY SYSTEMS, INC.  
Oak Ridge, Tennessee 37831-2008  
for the  
U.S. DEPARTMENT OF ENERGY  
under Contract No. DE-AC05-84OR21400

---

<sup>#</sup> Postdoctoral Research Associate of Oak Ridge Associated Universities

<sup>\*</sup> Energy Division

<sup>+</sup> Fusion Energy Division



3 4456 0380471 0



## TABLE OF CONTENTS

	<u>Page</u>
LIST OF FIGURES .....	v
ACKNOWLEDGEMENTS .....	ix
ABSTRACT .....	xi
1. INTRODUCTION .....	1
2. LITERATURE SURVEY .....	4
2.1 SCOPE OF THE REVIEW .....	4
2.2 THEORIES .....	4
2.3 RELEVANT RESEARCH WORKS IN THE PAST .....	5
3. NUMERICAL SIMULATIONS .....	7
3.1 ENERGY BALANCE EQUATIONS APPROACH .....	8
3.1.1 Physical Model .....	8
3.1.2 Governing Equations .....	8
3.2 NAVIER-STOKES EQUATIONS APPROACH .....	10
3.2.1 Magnetic Heat Pumping without Cooling Loads .....	10
3.2.1.1 Physical model .....	10
3.2.1.2 Governing equations .....	11
3.2.1.3 Discussion of results .....	13
3.2.2 Magnetic Heat Pumping with Cooling Loads .....	15
3.2.2.1 Physical model and basic assumptions .....	15
3.2.2.2 Discussion of results .....	16
3.3 OPTIMIZATION .....	19
3.4 CONCLUDING REMARKS .....	23
4. TEST SETUP AND EXPERIMENTAL RESULTS .....	25
4.1 REGENERATOR TUBE .....	25
4.1.1 Gadolinium Core .....	25
4.1.2 Regenerator Tube and Thermocouple Column .....	26
4.1.3 Working Fluid .....	27
4.1.4 Electric Heater as the Cooling Load .....	27

4.2 TEST SETUP .....	29
4.2.1 Test Stand .....	29
4.2.2 Driving Mechanism .....	30
4.2.3 Regenerator Tube Moving Speed .....	30
4.2.4 Magnet Field and System Control .....	31
4.2.5 Data Acquisition System .....	32
4.3 DATA ANALYSIS .....	32
4.3.1 Adiabatic Temperature Lift .....	32
4.3.2 Temperature Development in the Fluid Column .....	33
4.4 DISCUSSION .....	35
4.4.1 Reduction of Flow Thermal Mixing .....	35
4.4.2 Heat Transfer Enhancement of Gadolinium Core .....	36
5. CONCLUSIONS AND RECOMMENDATIONS .....	39
REFERENCES .....	41
Appendix A: The combined natural and forced convection in the regenerative tube flow of a magnetic heat pump .....	79
Appendix B: Experimental data .....	82

## LIST OF FIGURES

	<u>Page</u>
Fig. 3.1. Geometry of the flow .....	44
Fig. 3.2. Physical model of the regenerator tube in a magnetic heat pump with no heat exchangers present .....	45
Fig. 3.3. Gadolinium adiabatic temperature lift for 7-T from molecular field theory .....	46
Fig. 3.4. Temperature distribution in the regenerator fluid column after 10 cycles (validation of the computer code) .....	47
Fig. 3.5. Temperature color rasters in the regenerator fluid column with no heat exchangers present (Re=1630) .....	48
Fig. 3.6. Development of temperature distribution in the regenerator fluid column no heat exchangers present (Re=1630) .....	49
Fig. 3.7. Comparison of temperature distribution in the regenerator fluid column before and after dwelling .....	50
Fig. 3.8. Temperature color rasters in the regenerator fluid column with no heat exchangers present (Re=980) .....	51
Fig. 3.9. Development of temperature distribution in the regenerator fluid column with no heat exchangers present (Re=980) .....	52
Fig. 3.10. Comparison of the temperature distribution in the regenerator fluid column with no heat exchangers present between two flow cases, Re=1630 and Re=980 .....	53
Fig. 3.11. Physical model of the regenerator tube in a magnetic heat pump with heat exchangers present .....	54
Fig. 3.12. Temperature color rasters in the regenerator fluid column with heat exchangers present (Re=980) .....	55
Fig. 3.13. Development of temperature distribution in the regenerator fluid column with heat exchangers present (Re=980, after 12 cycles) .....	56

Fig. 3.14. Energy delivery rates from and to the hot and cold reservoirs after 12 cycles in the case of $Re=980$ .....	57
Fig. 3.15. Comparison of energy delivery rates as the function of charge time for flow rate cases of $Re=980$ and $Re=610$ .....	58
Fig. 3.16. Regenerator efficiency as a function of reduced length and reduced period (From ref. 29) .....	59
Fig. 4.1. Overview of the gadolinium core .....	60
Fig. 4.2. A thermocouples column in the regenerator tube. ....	61
Fig. 4.3. Overview of the reciprocating magnetic heat pump test setup .....	62
Fig. 4.4. Schematic of the reciprocating magnetic heat pump test setup. ....	63
Fig. 4.5. Overview of the regenerator tube with gadolinium core inside. ....	64
Fig. 4.6. Schematic of the superconducting pulse magnet dewar .....	65
Fig. 4.7. LabView IV for system monitoring and control. ....	66
Fig. 4.8. Measurement of gadolinium temperature lift of Brown's sample .....	67
Fig. 4.9. Measurement of gadolinium temperature lift of ORNL's sample .....	68
Fig. 4.10. Comparison of gadolinium temperature lift among samples .....	69
Fig. 4.11. Temperature development in the regenerator fluid column for the case of average $Re=300$ .....	70
Fig. 4.12. Temperature development along with the magnetic heat pumping processes at average $Re=300$ . ....	71
Fig. 4.13. Comparison of temperature development in the regenerator fluid column between experimental data and calculated values .....	72
Fig. 4.14. Comparison of maximum temperature spans among cases with different Reynolds number .....	73

Fig. 4.16. Two-speed transient regenerator tube flow of room temperature magnetic heat pumps .....	75
Fig. 4.17. Temperature distribution in the regenerator fluid column by using stepwise tube moving speeds of 0.04 and 0.02 m/sec .....	76
Fig. 4.18. Three dimensional geometry of flow problem .....	77
Fig. 4.19. Temperature color raster in a 3D regenerator fluid column .....	78
Fig. B1. Temperature development in the regenerator fluid column for the case of $Re=750$ with 15s-15s of cycle period .....	83
Fig. B2. Temperature development in the regenerator fluid column for the case of $Re=750$ with 30s-15s of cycle period .....	84
Fig. B3. Temperature development in the regenerator fluid column for the case of $Re=450$ with 25s-25s of cycle period .....	85
Fig. B4. Development of extreme temperatures in the regenerator fluid column for the case of $Re=300$ with 15s-37s of cycle period .....	86
Fig. B5. Development of extreme temperatures in the regenerator fluid column for the case of $Re=750$ with 15s-15s of cycle period .....	87
Fig. B6. Development of extreme temperatures in the regenerator fluid column for the case of $Re=750$ with 30s-15s of cycle period .....	88
Fig. B7. Development of extreme temperatures in the regenerator fluid column for the case of $Re=450$ with 25s-25s of cycle period .....	89



## ACKNOWLEDGEMENTS

The authors wish to thank Jim Luton, Tom Wilson and Bill Schwenterly for their help in operating the superconducting magnet. Thanks also to Mr. Vernon Latham, Mr. Gary Simon, Mr. Mike Willord, Mr. Frank Bunner and Mr. Francis Roach of Oak Ridge National Laboratory Y-12 plant supporting crew. The authors express their appreciation for the assistance of Mrs. Karen Treadway, Mrs. Mia Bunner and Mrs. Deborah Counce in report preparation. This work was a part of the Thermal Sciences Research Program activities at Oak Ridge National Laboratory sponsored by the Advanced Industrial Concepts Division, U.S. Department of Energy, under contract DE-AC05-84OR21400 with Martin Marietta Energy Systems, Inc.



## ABSTRACT

Transient flow phenomena in the regenerator tube of reciprocating magnetic heat pumps have been studied numerically and experimentally. In the numerical study, two approaches were taken: (1) solving the energy balance equations for fluid through a porous bed directly and (2) solving the Navier-Stokes equations with a buoyancy force term in the momentum equation. A flow thermal mixing problem was found in both approaches because of the piston-like motion of the regenerator tube that hinders the development of the temperature. The numerical study results show that a 45 K temperature span can be reached in 10 minutes of charge time through the use of a 7-Tesla magnetic field. Using the second numerical approach, temperature stratification in the regenerator fluid column was clearly indicated through temperature rasters. The study also calculates regenerator efficiency and energy delivery rates when heating load and cooling load are applied. Piecewise variation of the regenerator tube moving speed has been used in the present numerical study to control the mass flow rate, reduce thermal mixing of the flow and thus minimize the regenerative losses. The gadolinium's adiabatic temperature has been measured under 6.5 Tesla of magnet field and different of operating temperatures ranging from 285 K to 320 K. Three regenerative heat pumping tests have also been conducted based on the Reynolds number of the regenerator tube flow, namely  $Re=300$ ,  $Re=450$ , and  $Re=750$  without loads. Maximum temperature span are 12 K, 11 K and 9 K for the case of  $Re=300$ ,  $Re=450$  and  $Re=750$ , respectively. Experimental data are in good agreement with the numerical calculation results, and have been used to calibrate the numerical results and to develop a design database for reciprocating-type room-temperature magnetic heat pumps.



## 1. INTRODUCTION

The concept of the Magnetic Heat Pump (MHP) is based on the principle of the magnetocaloric effect of magnetic materials, in which entropy, and therefore temperature, changes when a material is magnetized or demagnetized. When a soft magnetic material is in its natural (i.e., zero magnetic field) state, the magnetic dipoles in the material are in a relatively disordered state; if a magnetic field is imposed upon the material, the dipoles align with the field and are transformed into an ordered state. A decrease in entropy (corresponding to an increase in temperature) occurs. Conversely, if a magnetic material is suddenly demagnetized by being removed from a magnetic field, an increase in entropy and a corresponding decrease in temperature will occur.

The origin of the concept of magnetic cooling can be traced back more than a half century to the 1920s, when Giauque<sup>1</sup> and Debye<sup>2</sup> independently proposed using the magnetocaloric effect of magnetic materials for refrigeration to produce ultra-low temperatures. In 1933, Giauque was able to achieve a cooling temperature of 0.5 K down from 3.5 K by using the magnetocaloric effect.<sup>3</sup> His method was to cool a paramagnetic salt to 3.5 K in a magnetic field and then to demagnetize it adiabatically to achieve 0.5 K. This adiabatic demagnetization method is a one-shot or single-step refrigeration process that does not provide continuous cooling. It is still being used in low-temperature physics experiments to create temperatures extremely close to absolute zero.

The possibility of building a heat pump using the magnetocaloric effect was apparently first suggested in 1949 by Daunt,<sup>4</sup> who combined two isothermal and two adiabatic magnetization and demagnetization processes to form a magnetic Carnot heat pump cycle that is capable of providing sustained cooling. However, laboratory experimentation was not conducted until 1975, when Brown built and tested a reciprocating magnetic heat pump assembly using gadolinium as the working medium.<sup>5</sup> Brown's study of MHPs was aimed primarily toward near-room-temperature space-conditioning applications. Since then, many experimental and analytical studies have been done on the heat pump concept, and the end-use applications vary

from 4 K in the liquid-helium temperature range, as in the study of magnetic refrigerators by Barclay,<sup>6</sup> to 400 K, as in the production of low-pressure steam for industrial heating by Idaho National Engineering Laboratory.<sup>7</sup>

Like the magnetic properties of materials, the temperature changes caused by the magnetocaloric effect are highly dependent upon a strong magnetic field. Strong fields created by superconducting magnets are often preferred and are probably necessary for many practical applications. The complexity and relatively high cost of traditional superconducting magnets (which must be cooled by liquid Helium) are among the factors that have affected interest in magnetic heat pump development. The discovery of high-temperature superconductivity shows promise not only for achieving higher magnetic fields than before, but also for offering a simpler and less costly superconducting magnet (which may be cooled by liquid N<sub>2</sub>). Continued advancement in superconducting materials research will enhance the viability of MHP technology as well. In view of the recent rapid progress in the superconductivity area, we have investigated many possible options for MHP concepts that could utilize the newly discovered materials and technology. A test rig for a superconducting MHP was assembled using an existing low-temperature superconducting magnet. This effort was supported internally by the ORNL Exploratory Studies Program. A noticeable temperature increase was achieved. However, the existing magnet is not designed for the pulse-DC mode of operation needed in the test setup. Sustained experimentation on regenerative magnetic heat pumping was not fulfilled in the initial internal research and development (R&D) study.

This report documents our study of the numerical and experimental studies of the transient flow phenomena in the regenerator tube, and the temperature development in the regenerator fluid column of an MHP. In the numerical study, two approaches were taken: (1) solving the energy balance equations directly and (2) solving the Navier-Stokes equations with a buoyancy force term in the momentum equation. The results, presented in graphic form, not only show the time-dependent temperature distribution inside the regenerator tube, but also compare the temperature span, energy delivery rate, and regenerator efficiency among the cases in terms of Reynolds number and cycle charge time. We found that two-stage mass flow control can solve

the thermal mixing problem of the flow caused by the reciprocating motion of the gadolinium core inside the regenerator tube. In the experimental study, the adiabatic temperature of the lift of the gadolinium core has been measured; results show only a 6.5 K temperature increase under 6.5 Tesla of magnet field and 297 K of initial gadolinium temperature. Nevertheless, three tests are being conducted under 6.6 Tesla of magnet field with different Reynolds numbers:  $Re=300$ ,  $Re=450$ , and  $Re=750$ . Thermal mixing of the flow and other heat losses are expected; this provides the opportunity to improve the system performance by enhancing the heat transfer rate in the gadolinium core and controlling the mass flow rate through the gadolinium core.

It was noticed that the heat transfer mechanism in the regenerator tube flow is a combined natural and forced convection (see Appendix A). Buoyancy force term is very important and should not be excluded from the governing equations. However, for the sake of convenience, Reynolds number will be used through this entire report to tell the difference among cases.

## 2. LITERATURE SURVEY

### 2.1 SCOPE OF THE REVIEW

A literature search was performed. Communication with people in this field through personal contacts also provided valuable up-to-date information.

Earlier work, that done before 1976, mostly involved the application of the magnetocaloric effect in the cryogenics field with temperatures close to absolute zero. It is only recently that MHPs have been considered for applications with a temperature range from 20 K to near room temperature,<sup>8</sup> such as hydrogen liquefaction, cooling of high-temperature superconducting devices, cooling of industrial chemical processes, industrial and domestic refrigerator, and air-conditioning. Our effort concentrates on this temperature range.

The current review is divided into several categories, including literature dealing with

- . theories about the MHP and
- . existing experimental data.

### 2.2 THEORIES

MHPs are an application of the "magnetocaloric effect" that some materials have in a magnetic field. Barclay provides a good summary of MHP theories.<sup>8</sup> The magnetic moment and its interaction with thermal and mechanical properties are basically adding the term "magnetic work" to the internal energy equation.<sup>8,9,10-13</sup> The entropy change associated with temperature and magnetic field can be considered in three respects: lattice entropy, electronic entropy, and magnetic entropy.<sup>14-16</sup>

. Lattice entropy, the entropy associated with the vibration of the molecules, is also a function of temperature. It is complicated to calculate because it involves the application of Debye temperature (which is a material property) and Debye function.<sup>14-16</sup>

. Electronic entropy, the kinetic entropy of the electrons, is a function of temperature.

. Magnetic entropy, is the entropy change caused by the spin of the molecules when the material is magnetized under the magnetic field. It involves the strength of the magnetic field, material properties, temperature, Curie point, and the application of Brillouin function.<sup>17,18</sup>

To calculate the performance of MHP system, all three entropy components must be considered. Besides, many heat transfer problems are involved in actual MHP systems. Reference<sup>10</sup> describes in detail two heat transfer models of a regenerative magnetic refrigerator. With some modification, these models can be used to calculate the performance of regenerative MHPs.<sup>19</sup> Some of the losses of MHP systems were discussed in reference.<sup>20</sup>

### **2.3 RELEVANT RESEARCH WORKS IN THE PAST**

For MHP systems near room temperature, information on heat capacities is limited. Brown and Papell tested a regenerative MHP with gadolinium as the core material and with an ethanol and water mixture as the regenerative fluid.<sup>21</sup> The system, under no load condition, managed to have an 80-K (from 248 K to 328 K) temperature differential between cold and warm ends of the fluid column after 50 cycles (with a cycle length of approximately 60 seconds per cycle). However, steady-state operation was not achieved.

Barclay et al. conducted the same experiment using a low Reynolds number and obtained

the greatest temperature span of 19 K in a single cycle.<sup>6</sup> In 1984, Kirol et al. studied the geometrical effect of gadolinium, the refrigerator material, upon heat pump performance for both reciprocating and rotary heat pumps.<sup>20</sup> Until recently, Chen et al. of Oak Ridge National Laboratory (ORNL) proposed a thermodynamics magnetocaloric energy conversion research program to investigate the thermodynamic cycle of the MHP further.<sup>22</sup>

In the many feasibility studies, several design concepts were discussed.<sup>11,20</sup> Brown provided several gadolinium core design concepts. Kirol et al. discussed in detail a baseline reciprocating machine and counterflow rotary MHP design concept.<sup>20</sup> Green et al. discussed the reducing regenerative losses by using a multi-stage mass flow rate control scheme.<sup>23</sup>

### 3. NUMERICAL SIMULATIONS

The temperature development and transient flow phenomena in the regenerator tube of an MHP have been numerically calculated in this study. Two approaches were taken: (1) solving the energy balance equations directly by using finite difference numerical scheme and (2) solving the Navier-Stokes equations with a buoyancy force term in the momentum equation by using the finite control volume concept. A flow thermal mixing problem was found in both approaches because of the piston-like motion of the regenerator tube that hinders the development of the temperature. The results, presented in graphic form, not only show the time-dependent temperature distribution of the regenerator fluid column, but also compare the temperature span, energy delivery rate, and regenerator efficiency among the cases in terms of Reynolds number and cycle charge time.

A 50% methanol and 50% water mixture was used as the regenerator fluid in this study of a computer simulation of the regenerator tube flow of an MHP. The thermal properties of this mixture are shown in Table 1. These data associated with the fluid flow rate and cycle length will be used to calculate the Reynolds number to distinguish among cases.

**Table 1. Thermal properties of the 50% methanol and 50% water mixture.**

Thermal property	50% Methanol + 50% Water
Density (kg/m <sup>3</sup> )	893.0
Dynamic viscosity (N·s/m <sup>2</sup> )	1.0466×10 <sup>-3</sup>
Thermal conductivity (W/m/K)	0.391
Thermal diffusivity (m <sup>2</sup> /s)	0.118×10 <sup>-6</sup>
Specific heat (J/kg/K)	3691

### 3.1 ENERGY BALANCE EQUATIONS APPROACH

#### 3.1.1 Physical Model

The geometry of the flow problem considered is shown in Fig. 3.1. A vertical cylinder 0.05 m in diameter and 1.0 m in height, perfectly insulated on the outside and at the base, was assumed. However, in following the first approach, we simplified the physical model into a one-dimensional vertical flow. Fluid properties, including density, were assumed to be independent of temperature.

#### 3.1.2 Governing Equations

The basic theory of thermal wavefront propagation through a porous bed was first presented by Schumann in 1929 (ref.24). The temperature span across the bed was considered small enough that the bed and gas properties could be taken as constant. Also, momentum and mass-continuity effects were ignored, leaving only a set of energy-balanced equations to describe the problem. The one-dimensional, partial differential energy equations are

$$\alpha \rho_f C_f \frac{\partial T}{\partial t} = -V_f \rho_f C_f \frac{\partial T}{\partial x} + h A (\theta - T) . \quad (1)$$

$$(1-\alpha) \rho_s C_s \frac{\partial \theta}{\partial t} = h A (T - \theta) + (1-\alpha) \lambda_s \frac{\partial^2 \theta}{\partial x^2} . \quad (2)$$

Initial condition and boundary conditions are as follows:

$$T = \theta = T_o , \quad t=0 ,$$

and

$$\frac{\partial T}{\partial x} = \frac{\partial \theta}{\partial x}, \quad x=0 \quad ,$$

$$\frac{\partial T}{\partial x} = \frac{\partial \theta}{\partial x}, \quad x=x \quad ,$$

$\alpha$  is the gadolinium core porosity,

$\rho_f, \rho_s$  are the fluid and gadolinium densities, respectively,

$C_f, C_s$  are the fluid and gadolinium heat capacities, respectively,

$V_f$  is the fluid flow rate,

$T$  is the fluid temperature,

$T_o$  is the initial fluid temperature,

$h$  is the conductance between the fluid and gadolinium,

$\theta$  is the gadolinium temperature,

$A$  is the contact area per unit volume of the bed,

$\lambda_s$  is the effective axial thermal conductivity of the bed.

The coupled nonlinear, partial differential Eqs.(1) and (2) that describe the one-dimensional processes in the porous magnetic bed can be solved only by numerical techniques. Calculations based on Eqs. (1) and (2) have been done by Chen<sup>22</sup> and Larson.<sup>25</sup> However, the results are

inadequate to describe the heat transfer phenomena in the reciprocating MHP system, because of the neglect of the body force term in the governing equations. Numerical calculation based on Navier-Stokes equations thus come to the stage. The details of modeling the reciprocating MHP system and solve the temperature field based on Navier-Stokes equations is shown in the next section.

## **3.2 NAVIER-STOKES EQUATIONS APPROACH**

### **3.2.1 Magnetic Heat Pumping without Cooling Loads**

#### **3.2.1.1 Physical model**

The physical model considered in this study is shown in Fig. 3.2. In the magnetization process, it was assumed that the gadolinium core remained at the top of the tube, allowing the fluid to flow from the top at a constant speed. There are three ways to transfer the heat from the gadolinium core to the fluid: constant heat generation rate, constant heat flux rate, and constant temperature lift. In the present study, the gadolinium temperature was set at a constant value with a specified increase above the initial fluid temperature; the increase is based on the calculation of mean field theory. The half-cycle time is set to allow the fluid to travel the entire length of the regenerator tube. In the demagnetization process, the gadolinium core remains at the bottom end of the tube, and the flow rises from the bottom at the same speed as before but in the opposite direction. At this point, the operating temperature surrounding the gadolinium core changes according to the temperature resulting from the previous magnetization process.

Modeling this sequential movement of the magnetization and demagnetization processes or "piston" movement is complicated in most computational fluid dynamics computer codes. Calculations were made by using FLUENT code.<sup>26</sup> Several assumptions have been made, including a constant fluid flow rate, constant fluid inlet temperature, constant gadolinium

temperature, and perfect insulation surrounding the tube. Another major assumption is the gadolinium temperature increase. The calculation is good enough to be two dimensional, and  $12 \times 20$  grid points are sufficient for both the laminar and the turbulent flow calculation because the flow field is changing mainly in the flow direction. One important technique in simulating this up-and-down gadolinium core movement inside the tube is adapting the previous set of data and running it for the next half-cycle after resetting all the boundary conditions.

### 3.2.1.2 Governing equations

The governing equations for this two-dimensional vertical channel flow can be written in the following Cartesian coordinate form:

$$\frac{\partial u}{\partial x} + \frac{\partial v}{\partial y} = 0 \quad . \quad (3)$$

$$\frac{\partial u}{\partial t} + u \frac{\partial u}{\partial x} + v \frac{\partial u}{\partial y} = -\frac{1}{\rho} \frac{\partial p}{\partial x} + \nu \left( \frac{\partial^2 u}{\partial x^2} + \frac{\partial^2 u}{\partial y^2} \right) + g\beta(T-T_0) \quad . \quad (4)$$

$$\frac{\partial v}{\partial t} + u \frac{\partial v}{\partial x} + v \frac{\partial v}{\partial y} = -\frac{1}{\rho} \frac{\partial p}{\partial y} + \nu \left( \frac{\partial^2 v}{\partial x^2} + \frac{\partial^2 v}{\partial y^2} \right) \quad . \quad (5)$$

$$\frac{\partial T}{\partial t} + u \frac{\partial T}{\partial x} + v \frac{\partial T}{\partial y} = \alpha \left( \frac{\partial^2 T}{\partial x^2} + \frac{\partial^2 T}{\partial y^2} \right) \quad . \quad (6)$$

$$p = \rho \left( \frac{R}{M} \right) T \quad . \quad (7)$$

where,  $u$  and  $v$  are the fluid velocities along and normal to the fluid flow direction,  $p$  is the

pressure,  $\nu$  is the dynamic viscosity of the fluid,  $g$  is the gravity,  $\beta$  is the thermal expansion coefficient of fluid and the symbol  $T_0$  represents the reference fluid temperature,  $\alpha$  is the fluid thermal conductivity,  $R = 4.187$  kJ/kg/K is the universal gas constant, and  $M$  is the average fluid molecular weight. The equations governing this fluid flow are based on mass, momentum, and energy conservation laws. The Boussinesq approximation has been applied to the buoyancy force term in the x-momentum equations, where density  $\rho$  can be computed by using the ideal gas law of Eq. (7). Equations (3)–(6) are solved subject to the following boundary conditions.

$$u, v, \frac{\partial T}{\partial y} = 0, \text{ on both walls.}$$

$$T = T_i, u = U_i, \text{ on channel inlets.}$$

$$P = 0, \text{ on channel outlets.}$$

The set of equations and boundary conditions presented earlier comprises the mathematical statement of the problem. A finite volume numerical method has been used to obtain the algebraic equations that govern the values of  $u$ ,  $v$ ,  $p$  and  $T$  at numerical grid points. The conservation laws expressed by Eqs. (3)–(6) are integrated over elemental control volumes centered around the grid points. The details of the numerical procedure are omitted because the methodology used here has been documented by Patankar.<sup>27</sup> A quadratic upwind differencing (QUICK) scheme was used to discretize the nonlinear convective term. This is a high-order scheme that offers reasonable stability characteristics. The coupled algebraic equations for flow and temperature variables are solved by a semi-implicit method known as "SIMPLE".<sup>28</sup>

The gadolinium adiabatic temperature lift as shown in Fig. 3.3 will be added to or

subtracted from the inlet fluid temperature in the beginning of each half-cycle. The resulting temperature then will be stored to the fluid by carrying the heated and cooled gadolinium core up and down through the regenerator fluid column to complete the magnetization and demagnetization processes of the reciprocating MHP cycles.

The computer code was validated using a 50% ethanol and 50% water mixture as the working fluid, with a tube moving speed of 0.05 m/s, under exactly the same simulated conditions as when Brown did the experiment in 1978. Figure 3.4 shows the temperature distribution after 10 cycles, in a case of Reynolds number is equal to 1850. The dimensionless quantity  $x^* = x/L$ , is a normalized tube height in the vertical axis of Fig. 3.4 illustrates the locations ( $x$ ) of the data points in the regenerator fluid column ( $L$ ). Results showed that the temperature distributions are in good agreement with each other.

### 3.2.1.3 Discussion of results

Following validation of the computer code, results were obtained for a vertical channel with an aspect ratio of 20. A  $12 \times 20$  numerical grid was used to solve the governing equations numerically.

Two different flow rate cases were simulated,  $Re = 1630$  and  $Re = 980$ , for tube moving speeds of 0.0333 m/s case and 0.02 m/s case, respectively. Here, Reynolds number is defined as  $Re = uD/\nu$ . For all cycles in these two cases, converged solutions were obtained in about 1000 iterations. About 800 iterations were required to run half-cycle to get a converged solution, and 200 iterations were allowed during the dwelling period.

Figure 3.5 (a) and (b) show the temperature contours inside the regenerator tube after 20 cycles (about 10 minutes of maintaining at high magnet field) for the case of  $Re = 1630$ . Figure 3.5 (a) shows the result of the magnetization process after 19.5 cycles. Figure 3.5 (b)

shows the result of the demagnetization process a half-cycle later, which is after 20 cycles. The warmest temperature was about 303 K after 20 cycles; the coldest fluid temperature at the bottom of the tube was about 258 K, making the total temperature span about 45 K.

Figure 3.6 shows the development of the temperature distribution in the regenerator fluid with no heat exchangers, presented after 10 and 20 cycles of the  $Re = 1630$  case. Thermal mixing was observed from the early stage of this run. There was a 9 K temperature difference between the magnetization and demagnetization processes in almost every cycle. The initial temperature zone was pushed away from the center of the tube after each half-cycle of the process.

The thermal mixing in the regenerator fluid can be observed easily by noting the intersections of the curves and the 283 K initial fluid temperature line in Fig. 3.6. After the demagnetization process, the initial temperature region was above the middle of the tube. But after the magnetization process, the initial temperature zone was pushed down from the middle of the tube. This flow mixing problem could be more severe in the actual experiment. To reduce this flow mixing problem, a longer tube could be used (or the moving tube speed slowed) or the heat transfer area per unit volume of gadolinium core could be reduced (this approach usually would not be desirable). The best alternative for solving the mixing problem seems to be slowing the moving speed of the regenerator tube.

Preliminary results of this numerical study show that 6 seconds of dwelling between half-cycles did help stratify the temperature field, which in turn reduced flow mixing to some extent. It was noticed that the dwelling period is necessary not only because it can reduce the flow mixing, but mainly because it provides time for the magnet field to ramp up and down to reach the desired magnetic field strength. Figure 3.7 shows a 1 K temperature decrease in the upper portion of the regenerator tube. That decrease indicates that the dwelling at the end of each half-cycle is necessary in running this MHP experiment. The 6 seconds dwelling period is adequate fine to stratify the density field, according to the observation from this numerical study. A longer dwelling period will cause more heat loss to the ambient.

Since decreasing the flow rate is a way to avoid fluid flow mixing in the regenerator tube, the second case was simulated by decreasing the tube moving speed from 0.0333 m/s to 0.02 m/s. Figures 3.8(a) and 3.8(b) show the temperature color rasters of the magnetization and demagnetization processes after 11.5 cycles and 12 cycles (about 10 minutes of maintaining at high magnet field), respectively. These two figures show a clear temperature stratification in the regenerator tube as good as in the previous case. However, the lower flow rate has reduced mixing to some extent. Consequently, the initial temperature of the 283 K zone is less pushed away from the center of the tube. Although the lower heat transfer rate accompanied the lower Reynolds number, the total temperature span was still about 43 K.

Figure 3.9 shows the development of the temperature distribution in the regenerator tube in the  $Re = 980$  case after 12 cycles. The temperature difference between the magnetization and demagnetization processes is about 6 K, which is 3 K less than the difference in the previous  $Re = 1630$  case. The temperature distribution is also more symmetric and uniform on both sides of the tube.

A comparison of the temperature distribution in the regenerator fluid column between the  $Re = 1630$  case and the  $Re = 980$  case after 20 minutes of cycling time is shown in Fig. 3.10. The temperature distribution in the lower portion of the tube in these two cases is quite close, indicating that in the  $Re = 1630$  case, the temperature on the cold side of the tube did not decrease as much as was expected. In other words, there is moderate thermal mixing in the high-Reynolds-number cases.

### **3.2.2 Magnetic Heat Pumping with Cooling Loads**

#### **3.2.2.1 Physical model and basic assumptions**

The physical model of the regenerator tube flow with heat exchangers presented in an

MHP is shown in Fig. 3.11. The model used in the previous cases was modified by adding heating and cooling coils to the top 10 cm and bottom 10 cm of the regenerator fluid column. In the magnetization process, both the initial operating temperature of the gadolinium and the fluid initial temperature are at 283 K. Fluid at a constant temperature of 303 K and 263 K is circulating in the heat exchangers installed at the top and bottom ends of the regenerator tube, respectively. Fluid travels from the top of the tube, passes through the gadolinium core, and reaches the bottom of the tube to finish the magnetization half-cycle. In the demagnetization process, the setup remains the same but the fluid flow direction is reversed.

### 3.2.2.2 Discussion of results

This is the MHP application with both heating load and cooling load attached to the regenerator tube. Heat exchanger coils were present at the top and 10 cm bottom of the regenerator fluid column.

To model the MHP with heating and cooling loads, the value of the heating and cooling loads first must be calculated. For instance, in the  $Re = 980$  case with the 50% methanol and 50% water mixture as the working fluid, if after 10 cycles the average fluid temperature at the top 10 cm of the tube is about 308 K, the heating rate will be about 20 W. The same method can be used to calculate the refrigeration rate in the other end of the regenerator fluid column. As an alternative, these two constant heat generation and dissipation zones can be assumed to be two constant temperature reservoirs— a 303 K heat reservoir and a 263 K cold reservoir— at the top and bottom of the fluid column, respectively.

According to Brown's discussion of his experiment in a 1978 paper, the experiment he ran was basically for heating load only. He inserted a heating coil into the top 10 cm of the

regenerator fluid column and allowed water at a temperature of 283 K at the inlet to circulate through the coil to simulate a constant heating load. When the experiment began, the fluid temperature was 258 K and the top 10 cm of the fluid column was maintained at 283 K. After 25 to 30 cycles of 60 seconds each, the fluid temperature at the top 10 cm of the regenerator tube was increased to 284 K, and heat was rejected into the heat exchanger coil where the heat extraction began. The coldest temperature decreased to about 241 K after the same period of time, 25 to 30 cycles.

In the computer model of the present study, we assumed two constant temperature regions at the top and bottom 10 cm of the regenerator fluid column, instead of two constant heat flux zones. The initial fluid temperature was 283 K, and the constant highest and lowest temperatures were 303 K and 263 K at the top and bottom of the regenerator fluid column, respectively. The objective of this simulation was to estimate the amount of time required for the regenerator fluid to pass its threshold temperatures and reach its steady state, if possible, or reach to its "pseudo-steady-state" if any interference occurred.

We had found that the lower the Reynolds number used to run the case, the less flow thermal mixing would occur. Therefore, in this study we started with  $Re = 980$ , which is a tube moving speed of 0.02 m/s or 50 seconds of half-cycle length without dwelling.

Note that the heating and cooling capacities do not have to be symmetric as the function of time; that is, one side of the fluid column can start delivering energy to the load while the other end is still developing its temperature and has not reached its threshold temperature. This is the characteristic of the gadolinium temperature increase, which is not a linear function of temperature. However, the heating and cooling capacity still can be calculated based on the temperature difference in these two extreme temperature regions. No matter how different these two values are, once a constant energy delivery rate is reached, no further calculation will be needed.

Preliminary results of this computer modeling show that the mass imbalance will occur

when we put threshold temperature zones on both ends of the tube at once. Thus, we must assign a constant temperature value to the 10-cm outlet zone after each half-cycle and use the average value of those temperatures as the initial temperature for the next half-cycle.

Figure 3.12 (a) and (b) shows the color rasters of the temperature distribution in the regenerator fluid column after 12 cycles for the magnetization and demagnetization processes, respectively. Note that the presence of the heat source and heat sink at the ends of the regenerator tube does accelerate the process to reach its extreme temperatures, if we compare with the same Reynolds number case of 980 without loads. However, the thermal mixing of the flow occurs in both loaded and unloaded applications because of the piston-like movement of the gadolinium core that carries unwanted fluid temperature to the outlet after each half-cycle of the process.

Figure 3.13 shows the development of the temperature field in the regenerator fluid column after 12 cycles in the case of  $Re = 980$ . The trend of the temperature development can be seen clearly. However, calculating the average outlet temperature became a problem, mainly because of the high temperature gradient surrounding the gadolinium core, especially with a constant temperature reservoir beside it. Overestimation of this average temperature is quite possible in this computer simulation.

The overestimation problem will mitigate over time when the temperature gradient in both ends of the tube becomes gradually smaller. It is worst at the beginning of the simulation when temperature changes are dramatic in the area between the gadolinium resting places and the threshold temperature zones. The method that we used in this study was to add 10% of the temperature at the upstream nodal points and 10% of the temperature at the downstream nodal points to 80% of the gadolinium core temperature, instead of just averaging with the surrounding temperature. This calculation scheme is based on observation of the preliminary results of this study.

Delivery of energy to the heating load through the heat exchanger coil at the top of the fluid column starts after 12 cycles. The average temperature at that time at the top 10 cm of the fluid column was about 304 K. Based on the temperature difference during this 50-second period of the demagnetization process, the energy delivery rate is about 7 W during the second-half-cycle of cycle 12. On the other end of the fluid column, refrigeration delivery is still developing; and the value is still on the negative side of  $-15$  W, which indicates that 15 W of energy has been supplied to the low-temperature reservoir during the entire cycle 12.

Figure 3.14 shows these two energy delivery rates as the function of the cycles. The delivery of energy to the heating load began shortly after 10 cycles, and the energy delivery rate kept increasing until slightly after 12 cycles. Then it reached its maximum and remained at a constant rate of 6 W. In the meantime, the lower temperature zone in the lower portion of the tube was still developing.

The same procedure was repeated using a Reynolds number of 610 for another case, which had a fluid flow rate of 0.0125 m/s and a cycle length of  $80.0 \times 2$  seconds. Figure 3.15 shows a comparison of energy delivery rates as the function of charge time for two cases,  $Re = 980$  and  $Re = 610$ . The lower the Reynolds number (or moving speed of the tube), the more quickly a steady state (or pseudo-steady-state) can be reached, and the higher the energy delivery rate that can be achieved. This indicates and confirms that the lower the flow rate, the less flow thermal mixing will occur in the regenerator fluid column during both the magnetization and demagnetization of an MHP.

### 3.3 OPTIMIZATION

The classical introduction to a deeper regenerator theory is the work by Hausen and Nusselt published in 1929 (revived by Jacob 1959). In the mathematical treatment of the

regenerator problem, Hausen developed a solution for a regenerator in which the thermal conductivity of the solid is zero parallel to the fluid flow and infinitely large normal to the fluid flow operating under cyclic steady state conditions.

A perfect gas flows at constant pressure through a regenerator matrix, first for a certain time in one direction and then for the same time in the other direction. The gas enters the regenerator at the temperature of the warm heat exchanger at constant temperature  $T_{hr}$ . When the gas flows in the other direction, it enters at the cold heat exchanger temperature  $T_{cr}$ . The temperature of the gas entering the warm space,  $T'_{hr}$ , will be slightly lower than the temperature  $T_{hr}$ . The temperature of the gas entering the cold space,  $T'_{cr}$ , will be slightly higher than the temperature  $T_{cr}$ .

If a constant  $C_p$  is assumed, a heat balance for the regenerator gives two characteristic temperature relations, or temperature deficits, for the gas:

$$\frac{T_{hr} - T'_{hr}}{T_{hr} - T_{cr}} = \frac{T'_{cr} - T_{cr}}{T_{hr} - T_{cr}} = 1 - \eta_{reg} \quad (8)$$

Hausen showed that these relations depend on two dimensionless variables,

$$\Lambda \equiv \frac{\alpha \cdot A_{Gd}}{\dot{m}_{Gd} \cdot C_{p,Gd}}, \quad \text{where } \Lambda \text{ is the reduced length of the regenerator,} \quad (9)$$

$$= \frac{(\text{Heat transfer coefficient}) \cdot (\text{Total heat transfer area})}{(\text{Total Gd mass passing each period}) \cdot (\text{Specific heat of the Gd})},$$

$$= \frac{[1.45 \text{ kW/m}^2/\text{K}] \cdot [0.1091 \text{ m}^2]}{[0.036 \text{ kg/s}] \cdot [0.2357 \text{ kJ/kg/K}]} = 18.64 ; \quad (10)$$

and

$$\Pi = \frac{\alpha}{C_f} \cdot P, \text{ where } \Pi \text{ is the reduced period,} \quad (11)$$

$$= \frac{(\text{Heat transfer coefficient})}{(\text{Heat capacity of fluid per area})} \cdot (\text{Time between flow reversals}),$$

$$= \frac{[1.45 \text{ kW/m}^2/\text{K}]}{[1.439 \text{ kJ/m}^2/\text{K}]} \cdot [25 \text{ sec}] = 25.19. \quad (12)$$

It is noted that in our reciprocating MHP system, gadolinium core (working medium) is passing through the 100% ethylene glycol (regenerator fluid) fluid column. Figure 3.16 (ref.29) shows one original graph by Hausen (taken from Jacob 1959). The generator efficiency can be read once the two parameters—the reduced length of the regenerator and the reduced period—have been calculated.

A calculation of the optimum regenerator geometry needs to take some practical considerations into account. The two most important phenomena are

- . heat conduction through the matrix and
- . flow maldistribution.

An optimization neglecting these phenomena will, for example, lead to a very short regenerator with a large front area.

Table 2 presents the regenerator efficiency for all the cases considered in this study. These values are all on the order of 0.70, which is quite good from the perspective of heat

exchanger effectiveness. However, regenerator efficiency still can be improved in two ways, based on the definition of reduced length of the regenerator and the reduced period. One way is to increase the total matrix surface area,  $A_{Gd}$ . The other is to prolong the time period for working medium, the gadolinium core to pass through the whole regenerator fluid column. For example, if we double the gadolinium contact area from 0.1091 m<sup>2</sup> to 0.2182 m<sup>2</sup> and prolong the cycle length from 25 seconds to 50 seconds, the regenerator efficiency will be increased from 0.67 to 0.72.

**Table 2. Regenerator efficiency as the function of Reynolds number in different applications**

Applications/Reynolds no.	A	II	Regenerator efficiency
Without loads/Re=980	18.6	25.2	0.70
Without loads/Re=1630	12.3	16.6	0.68
With loads/Re=610	22.4	30.2	0.71
With loads/Re=980	18.6	25.2	0.70
Energy equation/Re=1850	9.3	12.6	0.67

### 3.4 CONCLUDING REMARKS

Using the energy balance equations approach, we observed distorted temperature distribution in the regenerator fluid column because a constant fluid density was assumed and because of a flow mixing problem.

Using the approach of solving the Navier-Stokes equations for a regenerator fluid column without loads, temperature contours showed a clear pattern of temperature stratification inside the regenerator tube. Results also showed that reducing the moving speed of the tube could substantially reduce flow mixing without requiring excessive energy use to build up the total temperature span for the same charge time period. However, some engineering difficulties will accompany a low tube moving speed, including the inconsistency of regenerator tube traveling time between upward and downward due to gravity. These engineering difficulties must be tackled before the flow mixing problem in the regenerator fluid can be solved.

Constant temperature zones in the top and bottom 10 cm of the regenerator fluid column were assumed to be the heat source and heat sink, using in the approach of solving the Navier-Stokes equations for regenerator tube flow with loads. The results showed that constant energy delivery rates to both heating and cooling loads were achieved after a certain period of time, and that those rates then reached a pseudo-steady state because of flow mixing (the steady state is not real because it was forced by temperature mixing). To reduce the flow mixing to a minimum or to delay its occurrence in the early stage, the fluid temperature column must be built up slowly until it reaches the useful temperature range and then introduces the heat exchanger coils to the fluid column to extract energy from the regenerator tube (this will be different from Brown's experimental setup in 1978).

This study also has calculated regenerator efficiency and optimized the regenerator geometry. Reducing the moving speed of the tube, instead of extending its length, is an alternative for increasing regenerator efficiency. However, the efficiency value will be limited

to less than 0.2 because of the geometry of the regenerator tube of this reciprocating MHP.

No matter which result is treated as the standard to be used to compare with the experimental data, the existing flow mixing problem has to be minimized. The engineering difficulties accompanying the low tube moving speed, the short dwelling time, and the stability of the magnet field will be the challenges in the study of temperature development in the regenerator fluid column of an MHP.

## 4. TEST SETUP AND EXPERIMENTAL RESULTS

### 4.1 REGENERATOR TUBE

#### 4.1.1 Gadolinium Core

Table 3 shows the dimensions of gadolinium. The gadolinium core we used in this experiment is a grill of 5.08 cm diameter and 5.08 cm length. It consists of 28 parallel plates from 1.6 cm to 5.0 cm in width. The plates all have the same height, 5.08 cm, and same thickness, 0.1 cm. Careful measurement shows the total length of the gadolinium plates to be 107.4 cm. Thus, the total heat transfer area can be calculated as 0.1091 m<sup>2</sup>, and the total gadolinium volume can be calculated as 5.46×10<sup>-5</sup> m<sup>3</sup>. With the 7901 kg/m<sup>3</sup> of gadolinium density, we can calculate the total weight of the gadolinium core at about 431.4 g. However, the measured weight of these 28 gadolinium plates is 395.8 g. This difference tells us that we shaped almost 42.7 g from both ends of each gadolinium plate to prevent causing turbulent wake. Fig. 4.1 shows the overview of the gadolinium core in a 7.62-cm-high cylindrical stainless steel housing.

Table 3. The dimensions of gadolinium core

Description	Dimensions
Gadolinium plate thickness	0.1 cm
Gadolinium plate height	5.08 cm
Gadolinium plate total length	107.4 cm
Gadolinium housing inner diameter	5.08 cm
Gadolinium housing height	7.62 cm

#### 4.1.2 Regenerator Tube and Thermocouple Column

Figure 4.2 shows the dimensions of the regenerator tube and the locations of thermocouple points. The regenerator tube is a PVC tube of 5.08 cm diameter and 102 cm height with a rubber seal at the bottom of the tube and two suspension holes at the top. This tube could contain a fluid column up to 96.52 cm (38 in.) high. The thermocouple column is a 3/16-in. diameter tube with 7 copper-constantan thermocouple wires 6 in. even distance apart inside the tube. In order to install the thermocouple column in the regenerator tube and allow it to penetrate through the gadolinium core, we took 4 plates out from the center of the core.

Since the total installed gadolinium volume is  $V=5.46 \times 10^{-5} \text{ m}^3$ , the porosity of the gadolinium core can be calculated as

$$\text{Porosity } \alpha = 1 - \frac{V}{V'} = 1 - \frac{5.46 \times 10^{-5} \text{ [m}^3\text{]}}{\frac{1}{4} \pi (0.0508)^2 0.0508 \text{ [m}^3\text{]}} = 0.47 . \quad (13)$$

Heat flux and heat generation rates can be calculated based on the above data and with the 32 kJ/L of the gadolinium energy density. They are as follows (Assuming that the reciprocating moving rate is 0.02 Hz):

$$\text{Heat Flux } q = \frac{Q}{A} = \frac{32000 \times 0.0546 \times 0.02 \text{ [W]}}{0.1091 \text{ [m}^2\text{]}} = 320 \text{ [W/m}^2\text{]} . \quad (14)$$

$$\text{Heat generation rate } Q' = \frac{Q}{V} = \frac{32000(0.0546)0.02 \text{ [W]}}{5.46 \times 10^{-5} \text{ [m}^3\text{]}} = 0.64 \times 10^6 \text{ [W/m}^3\text{]} . \quad (15)$$

These two values plus the gadolinium temperature lift values become the three different inputs in the numerical analysis of the flow phenomena in the regenerator fluid column. The dimensionless locations of the 7 temperature sensors are 1/38, 7/38, 13/38, 19/38, 25/38, 31/38 and 37/38. This arrangement indicates that the fluid column height is 38 in. (96.52 cm), including the volume of the immersed gadolinium core, with the fluid level 2 in. from the top of the tube.

#### **4.1.3 Regenerator Fluid**

According to our numerical calculation results and all the relevant experimental data, the coldest fluid temperature in the regenerator tube will be around 246 K. Thus, the freezing point of the regenerator fluid has to be lower than this temperature. Ethylene glycol is the best among all the regenerator fluid candidates because of its easy availability. Table 4 shows the thermal properties of pure ethylene glycol, water, and the mixture of 50% ethylene glycol and 50% water. The mixture has a low freezing point of -37 °C (236.2 K) and moderately high specific heat and thermal conductivity compared with water.

#### **4.1.4 Electric Heater as the Cooling Load**

The calculation of the cooling load or heat output of the magnetic heat pump is based on the mass flow rate passing through the gadolinium core inside the regenerator tube. In a moderate Reynolds number case, we presume that the flow velocity is 0.1 m/sec, and the temperature lift or difference between tube and fluid is assumed to be 60 K in an hour.

**Table 4. Summary of thermal properties of the working fluid**

Thermal Property <sup>a</sup>	Ethylene glycol	Water	50% ethylene glycol + 50% water (by volume)
Molecular weight (g)	62.7	18.01	40.04
Density at 20 °C (kg/m <sup>3</sup> )	1113	998	1065
Freezing point (°C)	-12.7	0.0	-37.0
Kinematic viscosity (kg/m/s)	$23.262 \times 10^{-3}$	$0.993 \times 10^{-3}$	$4.260 \times 10^{-3}$
Dynamic viscosity (m <sup>2</sup> /s)	$20.9 \times 10^{-6}$	$1.0 \times 10^{-6}$	$4.0 \times 10^{-6}$
Specific heat (KJ/kg/K)	2.35	4.18	3.30
Thermal conductivity (W/m/K)	0.29	0.60	0.42

<sup>a</sup> Data from *ASHRAE 1989 Fundamentals Handbook (SI)*.

Therefore, with the thermal properties of the working fluid presented in Table 4, we will be able to calculate the cooling load as follows:

$$\begin{aligned}
 Q &= m \cdot C_f \cdot \Delta T && (16) \\
 &= [\rho A V_f] \cdot C_f \cdot \Delta T \\
 &= (1065 \text{ [kg/m}^3\text{]} \cdot \frac{\pi}{4} (0.05)^2 \text{ [m}^2\text{]} \cdot 0.1 \text{ [m/s]} \cdot (3.30 \text{ [kJ/kg/K]}) \cdot (\frac{60}{3600} \text{ [K]}) \\
 &= 0.0115 \text{ [kJ/sec]} \\
 &= 11.5 \text{ [W]} .
 \end{aligned}$$

There is a tremendous heat loss from the regenerator fluid column to the surrounding area because the superconducting magnet has to be operated under extremely cold conditions. Liquid helium is used to provide the cold working conditions. Thus, we have to take this heat loss into consideration in designing a heater for simulating the cooling load in an MHP. According to the above calculation and discussion, we chose a 50-W electric heater. It is an immersion type of heating device, and it was attached to the rubber seal at the bottom and inside of the regenerator tube. With a variable electric resistance device, we were able to adjust the heater output at different levels from 10 W to 50 W along with the different MHP cooling loads.

We have designed a electric heater in this study to simulate the MHP system cooling load. However, due to the unexpected low temperature lift of the gadolinium sample that we have measured in the laboratory, no experiment with cooling load has been conducted in the present study.

## **4.2 TEST SETUP**

The test setup of this reciprocating MHP consists of the test stand, driving mechanism, system control, and data acquisition system. Fig. 4.3 shows the overview of this test setup.

### **4.2.1 Test Stand**

Figure 4.4 shows the schematic of this reciprocating MHP test setup. The test stand is an 8-ft-high, 8-ft-wide and 6-ft deep wood frame, providing enough space to install the regenerator tube and conduct maintenance before and after each test. The superconducting magnet is installed on the basement floor in a 6-ft-tall dewar housing. The dewar protrudes 2.5 ft through the first floor. This setup allows us to operate everything on the first floor.

### **4.2.2 Driving Mechanism**

The driving mechanism consists of a motor and gear assembly, a pulley, a cable, and a variable speed controller. The motor and gear assembly is mounted upside down on the top of the test frame as shown in Figs. 4.3 and 4.4. The pulley has 4 in. of pitch diameter, which allows the cable to wrap up and release down in 3.75 turns, and allows the regenerator tube to travel 33.25 in. up and 33.25 in. down (the total fluid column is 38 in. high).

### **4.2.3 Regenerator Tube Moving Speed**

Regenerator tube moving speed is the most important parameter in the study of the reciprocating MHP. This speed will be used to decide the fluid mass flow rate through the gadolinium core and thus to calculate the Reynolds number to distinguish among cases.

Although the fluid column is 38 in. high, including the immersion of the gadolinium core, the center of the gadolinium core has to be set 2.5 in. from the upper fluid level and 2.5 in. from the bottom of the tube because of engineering design concerns about malfunctioning of the motor in reverse motion. The distance between the upper and lower limiting switch is therefore set at approximately 33.25 in. Using this total traveling distance, the regenerator tube moving speed can be decided by adjusting the variable speed controller, followed by the calculation of the Reynolds number for each case and the setup of the test matrix.

Figure 4.5 shows the overview of the regenerator tube with gadolinium core inside. Note that the gadolinium core has to be fixed at the top of the magnet dewar with two metallic rods welded on to the side of the gadolinium housing, allowing the regenerator tube along with the thermocouples column to move up and down through the gadolinium core.

#### 4.2.4 Magnet Field and System Control

The magnet we used in this experiment is a pulsed dc superconducting magnet. It has a bore of 9.0 cm (3.5 in.), an outer diameter of 21 cm (8.3 in.), and a length of 30.5 cm (12 in.). It is designed to produce an 8-T DC field at a current density of 12 kA/cm<sup>2</sup>. A dewar as shown in Fig. 4.6 with a reentrant warm bore can provide a 6.3 cm (2.5 in.) bore clear through the working space for the sample. The field uniformity is within 95% in the 10-cm (4-in.) long working space.<sup>22</sup>

The synchronization between the moving regenerator tube and the magnetization and demagnetization processes of the magnet field is the most important control factor among any other control schemes in the MHP. When the regenerator tube travels to the upper position (gadolinium core is at the bottom of the fluid column), the upper limiting switch tells the magnet to start to ramp down from the high field. It takes 15 seconds to ramp down to the zero field; it then holds at zero field and lets the regenerator tube travel down until it hits the lower limiting switch. At this time, the limiting switch signals the magnet to start ramping up from zero field to the highest field possible in 15 seconds; the magnet field then holds at high field and lets the regenerator tube travel up until it hits the upper limiting switch to finish a complete cycle. This synchronized motion has to be very precise through the entire test. Any other control failure hinders the temperature development in the regenerator fluid column.

The 15 seconds of dwelling period might be the major deficit in the temperature development in the fluid column, because the whole system is operating under extreme cold conditions. Any time delay will cause severe heat loss to the surroundings. The alternative way to avoid this heat loss is to shorten this dwelling period from 15 seconds to 10 seconds, or even to 6 seconds, disregarding the strength of the magnetic field.

Emergency shutdown of the magnetic field and the moving regenerator tube is manually controlled near the experimental site in case of any emergency.

#### **4.2.5 Data Acquisition System**

The LabView IV computer software is used to monitor this reciprocating MHP test system. The voltage, the strength, the current, and the temperature of the magnetic field are monitored on the computer screen. Temperature data through the regenerator fluid column also are scanned every 5 seconds, stored in the computer memory, and displayed on the computer monitor. Figure 4.7 shows all the major parameters monitored on the computer screen.

### **4.3 DATA ANALYSIS**

#### **4.3.1 Adiabatic Temperature Lift**

The adiabatic temperature lift of gadolinium has been measured in the Magnet Laboratory of the Fusion Energy Division of Oak Ridge National Laboratory under 6.5 Tesla of magnetic field and different operating temperatures ranging from 285 to 320 K. Two gadolinium plates were taken out from the core and sandwiched together with a thermocouple wire between the two plates. To prevent any condensation during the test, the sandwich was sealed with a Teflon tape. To avoid any heat loss to the ambient, the sample also was put in a well-insulated container. After the sample was frozen (in a freezer) down to 285 K or heated up (by a heat gun) to 320 K, it was placed near the center of the magnet (the magnet will center the sample automatically when the field is on), and tests were conducted over time to measure the heat absorbed by or dissipated from the gadolinium sample plates. Fig. 4.8 shows the result of a typical test of Brown's sample plates after preheating to 320 K with no water used. An adiabatic temperature lift of 6.5 K was found near 297 K initial gadolinium temperature under 6.5 Tesla of magnetic field. Fig. 4.9 shows the result of another similar test of the ORNL sample after precooling to 285 K. A 7.0 K adiabatic temperature lift was found near 293 K initial gadolinium temperature under the same magnetic field of 6.5 Tesla. Tests were conducted from a low temperature of 285 K to a high temperature of 320 K. Fig. 4.10 shows the comparison of the

gadolinium adiabatic temperature lift among samples as the function of initial temperature. Note that both Brown's sample and the ORNL sample have a factor of one-half the theoretical value because of their impurity and because of their being oxidized. It is estimated that the temperature span in the fluid column will be small after a long period of time. Nevertheless, three tests at  $Re=300$ ,  $Re=450$ , and  $Re=750$  are being conducted in the laboratory (Table 6). In order to minimize the flow thermal mixing, higher viscosity fluid of 100% ethylene glycol was used in the experiment. The results will be compared with the numerical calculation results based on the measured gadolinium adiabatic temperature lift of the gadolinium. Test results in graphic form will be shown in this section, followed by a discussion of the reduction of thermal mixing of the flow and the heat transfer enhancement of the gadolinium core.

#### 4.3.2 Temperature Development in the Fluid Column

Temperature development in the fluid column of a regenerative heat pump provides information about how the reciprocating MHP works. Combined natural and forced convection heat transfer (see Appendix B) takes place inside the regenerator tube. The moving gadolinium

**Table 5. Test matrix for ORNL reciprocating magnetic heat pumps**

Test (0 and 7 Tesla)	Flow rate (m/s)	Cycle period (s)	Cooling loads
Re=300	0.0243(0.90/37)	(15+37)×2	No
Re=450	0.0360(0.90/25)	(25+25)×2	No
Re=750	0.0600(0.90/15)	(30+15)×2	No
Re=750	0.0600(0.90/15)	(15+15)×2	No

The calculation of the Reynolds number is based on the property of 100% ethylene glycol.

core (relative to the working fluid) carries the energy along the tube; then the buoyancy force takes over and stratifies the fluid column into temperature sectors, with high temperatures on the top and low temperatures on the bottom of the column. Theoretically, there is no limitation to the development of temperature in the regenerator tube: as long as the magnetization and demagnetization processes continue, the temperature will keep decreasing to absolute zero. However, flow thermal mixing and heat loss to the ambient will hinder the development of temperature. Fig. 4.11 shows the temperature development in the regenerator fluid column at average  $Re=300$  with about 23 regenerative heat pumping cycles. A 5.3 K temperature span was developed right after the first cycle, then it gradually increased with constant heating and cooling rate to 12 K after 16 cycles. Flow thermal mixing occurred through the entire test and hindered the development of the temperature field after 20 cycles of the magnetic heat pumping processes. Fig. 4.12 is a close-up of a segment (from 15 min to 20 min) of the temperature development during the processes. The flow thermal mixing phenomenon can be seen very clearly in this experimental result because of the oscillation of the minimum and maximum fluid temperatures. The trend of the temperature development in the regenerator fluid column has been predicted in a so-called adaptive model shown in the Chapter 3 of this report. Fig. 4.13 shows the comparison of temperature development at  $Re=300$ ; the experimental data are in good agreement with the calculated values. Two tests at  $Re=450$  and  $Re=750$  have been also conducted in this study (see Figs. B1–B3 in Appendix B) with cycles of 25s-25s-25s-25s and 15s-15s-15s-15s, respectively. Maximum temperature spans of 11 K and 9 K (see Figs. B4–B7 in Appendix B) have been found in the cases of  $Re=450$  and  $Re=750$ , respectively. The difference in the temperature span implies that the faster the regenerator tube moving speed, the more serious the flow mixing that occurs. Another test at  $Re=750$  with a longer dwelling time in cycles of 30s-15s-30s-15s has been conducted to show that holding the constant field at both ends of the regenerator fluid column will allow enough time to release heat to or absorb the heat from the fluid. Results show the temperature span could have been about 1.0 K higher with a longer dwelling time. Fig. 4.14 shows the maximum temperature span versus time of all four cases. The lower the tube moving speed, the higher the temperature span that can be reached; and the longer the dwelling time, the higher and more stable the temperature span that will occur.

## 4.4 DISCUSSION

### 4.4.1 Reduction of Flow Thermal Mixing

The temperature span in the regenerator fluid columns of MHPs can be increased by continuous multistaging. The heat losses associated with the regenerative cycle are called regenerative losses or flow mixing heat losses in our previous numerical study. These flow thermal mixing heat losses cannot be easily controlled because of the continuous flow of the convecting fluid and the continuous magnetic field.

According to the discussion of the G. F. Green et al. report, "Mechanically Static Magnetic Refrigerator" of September 1991.<sup>30</sup> Management of the losses in the regenerative cycle requires coordination of the mass flow rate and the change of the magnetic field. Either of those elements would reduce the losses. However, the change of the magnetic field during fluid flow would complicate the heat transfer analysis because it would create too many different thermodynamic cycles. Therefore, the control of the mass flow rate of the fluid becomes the ultimate candidate for reducing the regenerative losses and thus solving the heat losses problem caused by the "flow thermal mixing" in our previous computer simulation.

Multistaging control of the mass flow rate of the fluid has been adopted in another numerical study. Figure 4.15 shows the two-stage velocity profile along the flow direction,  $y$ . The total gadolinium core traveling distance is 90 cm. Assuming that the velocity can be built up quickly to 0.04 m/sec in a very short time, when the gadolinium core reaches the 45-cm mark, the velocity will be slowed to 0.02 m/sec and remain constant for the rest of the half-cycle. The second stage of this half-cycle is very important, because reduction of the mass flow rate through the gadolinium core is needed to prevent flow thermal mixing and thus minimize some of the regenerative losses.

Since the FLUENT code<sup>26</sup> is using piecewise or profile velocity boundary conditions, it cannot be used along the flow direction, but only at the inlet. The preliminary study results

show that the FLUENT code could not be used in any case with time-dependent velocity boundary conditions. Thus, the simulation has to be modified as two-stage (equal tube length or so-called equal traveling distance) with different velocity and temperature boundary conditions at the tube inlet. Change of magnetic field may also be considered at this time in this model, since in the beginning of the second stage, both velocity and temperature boundary conditions have to be reset. However, considering the transition zone during the ramping of the magnetic field might be too long to lose to the ambient. Only a two-stage flow control mechanism was used in the present numerical study. Fig. 4.16 illustrate this model. The second-stage gadolinium temperature is adopted from the first stage outlet fluid temperature, and its inlet temperature is the second stage fluid temperature of the previous half-cycle.

Note that the total cycle length has to be recalculated for use in the FLUENT code. Based on the velocity profile, the calculated total cycle length is about 33.75 seconds. From acceleration to constant speed to a sudden stop, the average regenerator tube moving speed is 0.0267 m/sec, and the average Reynolds number associated with this speed is  $Re=1300$ .

Figure 4.17 shows the calculated of temperature distribution in the regenerator fluid column after 10 cycles of operation. The temperature difference between the magnetization and demagnetization process at the same location on the fluid column is no longer large compared with the single-stage model. Flow thermal mixing has been substantially reduced, and the temperature span reached up to 45 K after 10 minutes of charge time. Although no other heat loss agent was considered in this numerical study, including heat loss to the ambient, the result does show a promise for reducing the flow thermal mixing.

#### **4.4.2 Heat Transfer Enhancement in Gadolinium Core**

The conventional shapes of the gadolinium core in the reciprocating MHPs are either flat plates or porous particles inside a cylinder without any heat transfer enhancement agents or considerations. In the present numerical study, we emphasized increasing the heat transfer

capability per unit volume of gadolinium with a fixed value of porosity by modeling different shapes and arrangement of the gadolinium core.

In order to increase heat transfer area per unit volume and to increase the heat transfer coefficient, thin spiral concentric gadolinium rings were chosen in this study. The numerical simulation started with modeling a cylindrical ring concentrically immersed in a tube filled with fluid. The gadolinium ring is 0.004 m in diameter, 0.05 m long, and 0.005 m thick with polished surfaces on both sides, and is sunk in a 0.0508-m-diameter, 1.0-m-long regenerator tube filled with a 50% ethylene glycol and 50% water mixture. Fig. 4.18 shows the three dimensional geometry of this flow problem in the magnetization and demagnetization processes. To model ten or more shells of concentric rings requires many nodal points in the radial direction of the calculation domain if we are going to add ribs to the surface of each shell. Consequently, it will take more computer CPU time to simulate the piston-like movement of a reciprocating MHP, compared with the two-dimensional study. However, multiplying the number of rings by the one annulus result, neglecting the three-dimensional effect might give us a whole picture of this flow problem. Alternatively, the model will be focused on the enhancement of heat transfer between the fluid and the gadolinium core only, instead of modeling the gadolinium core running through the entire tube. The result will be the comparison of the overall heat transfer coefficient among the different shapes and arrangements of the gadolinium core.

The assumption we have made in the previous two-dimensional numerical study was that the gadolinium core temperature is a  $\Delta T$  above or below the surrounding fluid temperature in the beginning of each magnetization and demagnetization process. In the present study for a concentric type of gadolinium core, we adopted the constant heat generation rate assumption, which is based on the 32 kJ/L (or 4.050 J/g) of gadolinium energy density for a magnetization process from 0 to 7 Tesla. Fig. 4.19 shows the color raster of temperature development in a three-dimensional regenerator fluid column. Three-dimensional effect could not be seen very clearly in this figure, especially in the core region. Nevertheless, the investigation of this three-

dimensional full tube flow problem, in addition to the heat transfer enhancement in the gadolinium core, will be included in the third-phase effort of this project.

## 5. CONCLUSIONS AND RECOMMENDATIONS

The regenerative heat pumping performance of gadolinium was studied numerically and experimentally. The main objective of this study was to investigate temperature development in the regenerator fluid column and its associated heat transfer mechanism. The following are the conclusions of this work and the recommendations for the next phase.

### Conclusions

1. A flow thermal mixing problem in the regenerator tube was found in the numerical simulation in two different approaches: solving the energy balance equations and solving the Navier-Stokes equations.
2. Buoyancy force term cannot be excluded from the governing equations in any numerical attempt. Natural convection and forced convection heat transfer have the same order of magnitude in most cases of the temperature development in the regenerator fluid column of reciprocating MHPs.
3. Temperature stratification has been found clearly in the numerical simulation.
4. A temperature span of 45 K has been calculated in a typical case of  $Re=1630$  with no heat exchangers present after 20 cycles. This is based on the theoretical adiabatic temperature lift of gadolinium which has a maximum value of 14 K near 293 K of Curie temperature. However, the flow thermal mixing hinders the development of the temperature field.
5. Experimental results show that a 12 K temperature span was reached in a case of  $Re=300$  with a 15s-37s cycle period in about 16 cycles after it reached its pseudo-steady state condition. Low temperature spans are mainly due to the oxidation of the gadolinium plate. The adiabatic temperature lift of gadolinium has also been tested in the laboratory.

6. Numerical calculation results based on the measured gadolinium temperature lift are in good agreement with the experimental data. Both results show that the longer the dwelling time and the slower the regenerator moving speed, the higher the temperature span will rise.

### **Recommendations**

1. The control of mass flow rate is a good candidate approach to reducing the flow thermal mixing problem, according to a preliminary numerical study.

2. System heat loss to the ambient should be investigated further to ensure the accuracy of prediction of the temperature development in the regenerator fluid column.

3. The shape and arrangement of the gadolinium core should be studied carefully in the next phase to enhance the heat transfer capability from the gadolinium core to the fluid.

4. More experimental cases have to be run to collect enough data to predict the heating and cooling capacity as the function of reciprocating mass flow rate, or magnetic field.

5. A design data base for the MHP, including its system design and numerical predicting scheme, must be established in the near future.

## REFERENCES

1. Giauque, F., *Journal of American Chemistry Society*, Vol. 49 (1870).
2. DeBye, P., *Annual Physik*, Vol. 81, 1154- (1926).
3. Giauque, F. and D. P. MacDougall, *Physics Review*, Vol. 43, 768- (1933).
4. Daunt, J. G. and C. V. Heer, *Physics Review*, Vol. 76, 854- (1949).
5. Brown, G. V., *Journal of Applied Physics*, 47 (8) 3674-, (1976).
6. Barclay, J. A. and W. A. Stegert, "Magnetic Refrigerator Development," EPRI Report EL-1757, 1981.
7. Mills, J. I. et al., "Magnetic Heat Pump Cycles for Industrial Waste Heat Recovery," Proceedings, 19th IECEC, pp. 1369-, 1984.
8. Barclay, J. A., "Magnetic Refrigeration: A Review of a Development Technology," *Advances in Cryogenic Engineering*, Vol. 33, pp. 719-731, ed. R. W. Fast, Plenum Press, 1987.
9. EA-Mueller, Inc., "Cost and Availability of Magnetic Heat Pump Materials," EA-M Project 87-604-98 Report, prepared for U. S. Dept. of Energy, Office of Industrial Programs, Jan. 1989.
10. Callen, H. B., *Thermodynamics*, Wiley, N.Y., 1959.
11. Stratton, J. A., *Electromagnetic Theory*, Chapter 11, McGraw Hill, N. Y., 1941.
12. Barclay, J. A., "The Theory of an Active Magnetic Regenerative Refrigerator," Proceedings of Second Biennial Conference on Refrigeration for Cryogenic Sensors and Electronic Systems, Goddard Space Flight Center, Greenbelt, Md., Dec. 7 and 8, 1982.
13. Larson, A. V. et al., "Feasibility Analysis of Reciprocating Magnetic Heat Pumps," Semiannual Status Report for the Period 7/3/85 to 1/2/86 to NASA, Georgia Institute of Technology, Atlanta.
14. Brown, G. V., "The Practical Use of Magnetic Cooling," pp. 587-592 in Proceedings of 13th International Congress of Refrigeration, International Institute of Refrigeration, Washington, D. C., 1971.
15. Brown, G. V., "Magnetic Heat Pumping Near Room Temperature," *Journal of Applied Physics*, 47 (8) 3673-3680 (1976).

16. Oesterreicher H. and F. T. Parker, "Magnetic Cooling Near Curie Temperature Above 300 K," *Journal of Applied Physics*, **55** (12) 4334-4338 (1984).
17. Morrish, A. H., *The Physical Principles of Magnetism*, pp. 70-73, Wiley, 1965.
18. Brown, G. V., "Magnetic Stirling Cycles — A New Application for Magnetic Materials," *IEEE Transaction on Magnetics*, **13** (5), 1146-1148 (1977).
19. Chen, F. C., "Study of Superconducting Magnetic Heat Pumping," Oak Ridge National Laboratory, unpublished data, Oct. 1989.
20. Kirol, L. D. et al., "Magnetic Heat Pump Feasibility Assessment," EGG-2343 Report, prepared for DOE, EG&G, Idaho Falls, Idaho, 1984.
21. Brown, G. V. and S. S. Papell, "Regeneration Tests of a Room Temperature Magnetic Refrigerator and Heat Pump," National Aeronautics Space Administration, Lewis Research Center, prepared for *Applied Physics Letters*, March 10, 1978.
22. Chen, F. C., R. W. Murphy, V. C. Mei, G. L. Chen, J. W. Lue, and M. S. Lubell, "Loss Analysis of the Thermodynamic Cycle of Magnetic Heat Pumps," Phase I Final Report of Thermal Sciences Research Program on Thermophysics of Magnetocaloric Energy Conversion, ORNL/TM-11608, Feb. 1991.
23. Green, G. F., G. Patton, J. W. Stevens and J. C. Humphrey, "Magnetocaloric Refrigeration," DTNSRDC Report 87/032, March 1987.
24. Schumann, T. E. W., "Heat Transfer, A Liquid Flowing through a Porous Prism," *J. Franklin Institute*, Vol. 208, pp. 405-, 1929.
25. Larson, A. V. et al. "Feasibility Analysis of Reciprocating Magnetic Heat Pumps." Semiannual Status Report for the period of 7/3/1985 to 1/2/1986, NASA Research Grant NAG 3-600. Georgia Institute of Technology, Atlanta, Georgia
26. FLUENT Manual, TN-369, Rev.3, Creare Inc., 1987, Hanover, New Hampshire.
27. Patankar, S. V., "Numerical Heat Transfer and Fluid Flow," Hemisphere, Washington, D. C., 1984.
28. Patankar, S. V. and D. B. Spalding, "A Calculation Procedure for Heat, Mass and Momentum Transfer in Three-dimensional Parabolic Flows," *International Journal of Heat and Mass Transfer*, Vol. 15, 1787-1806 (1972).
29. Lundqvist, P., "The Real Stirling Cycle," Chapter 5 in *Stirling Cycle Heat Pumps and Refrigerators*, Ph.D. thesis, pp.117-122, 1992.

30. Green, G. F. et al., "Mechanically Static Magnetic Refrigerator," DTRC-PAS-91-42, Sep. 1991.

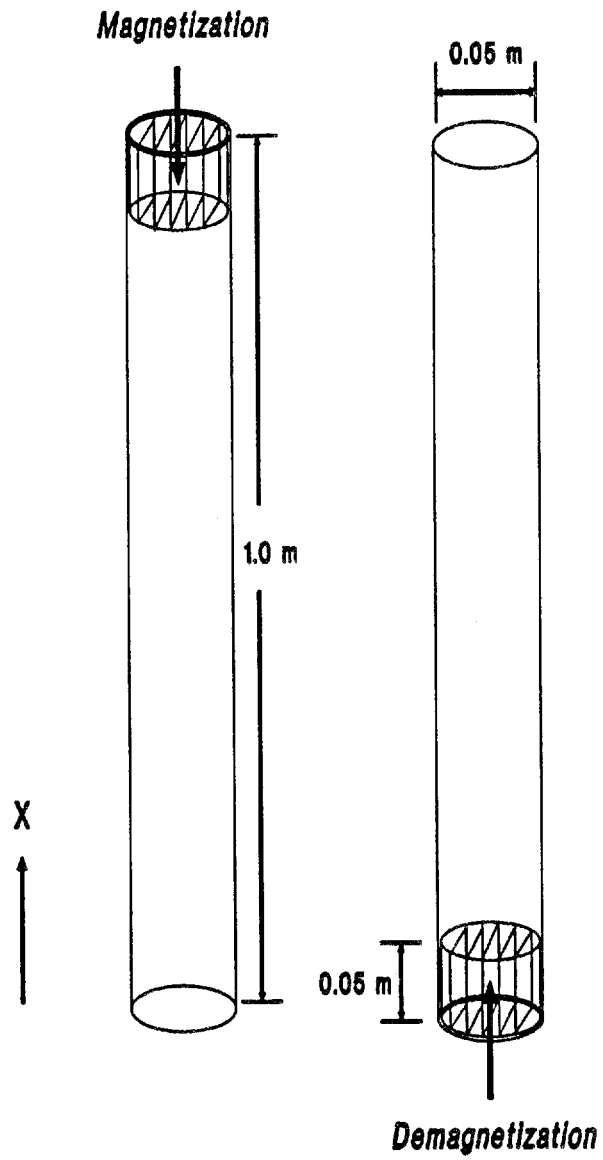


**Fig. 3.1. Geometry of the flow problem.**

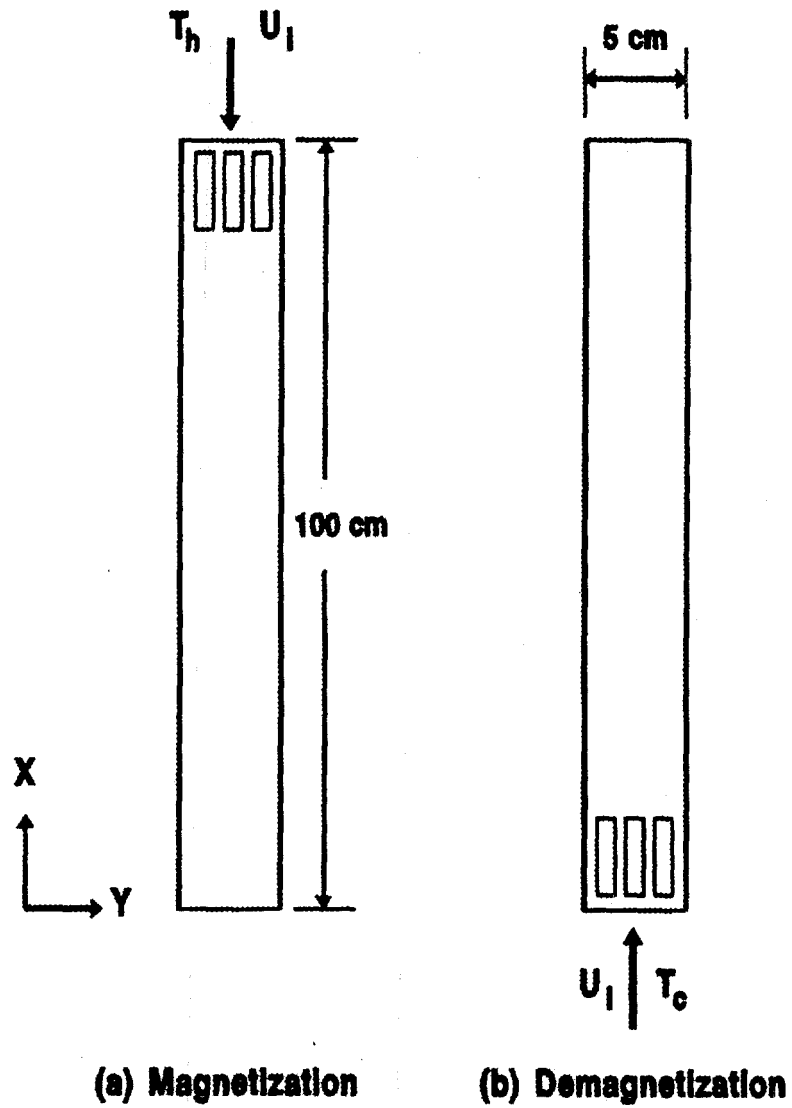
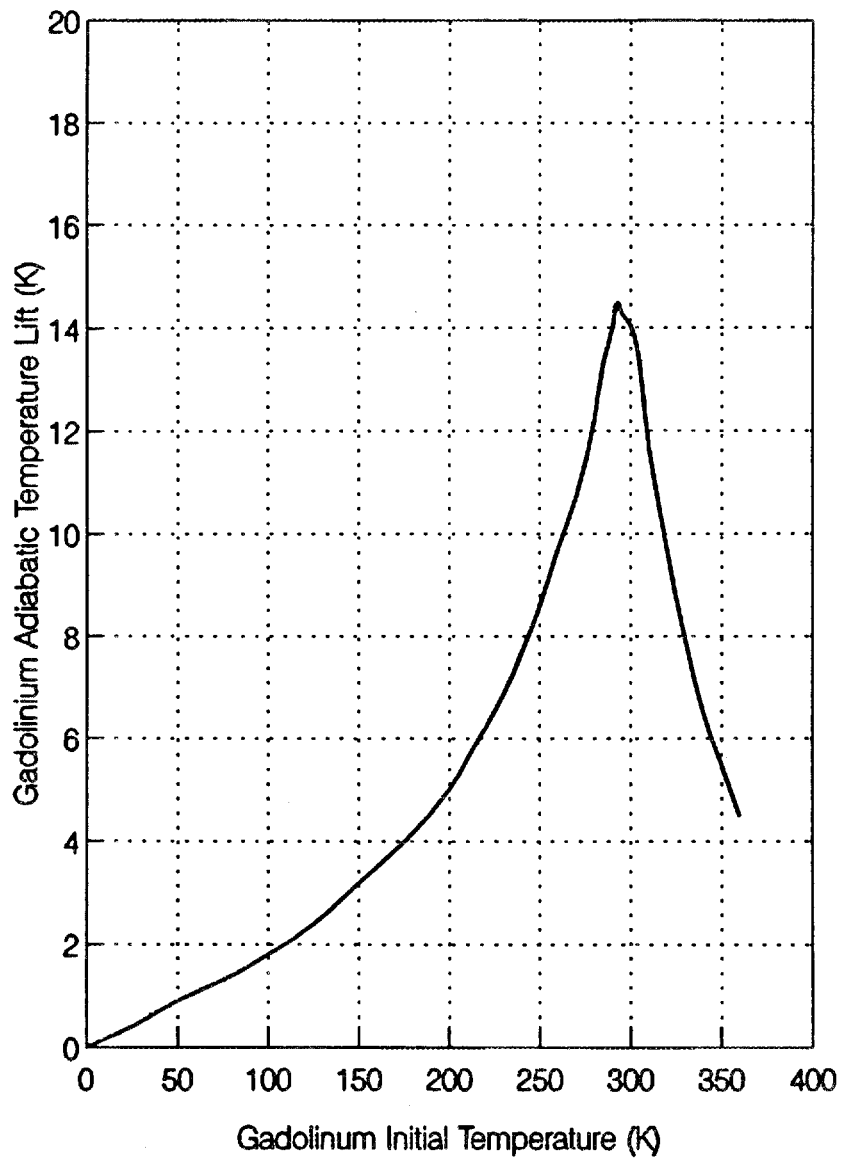
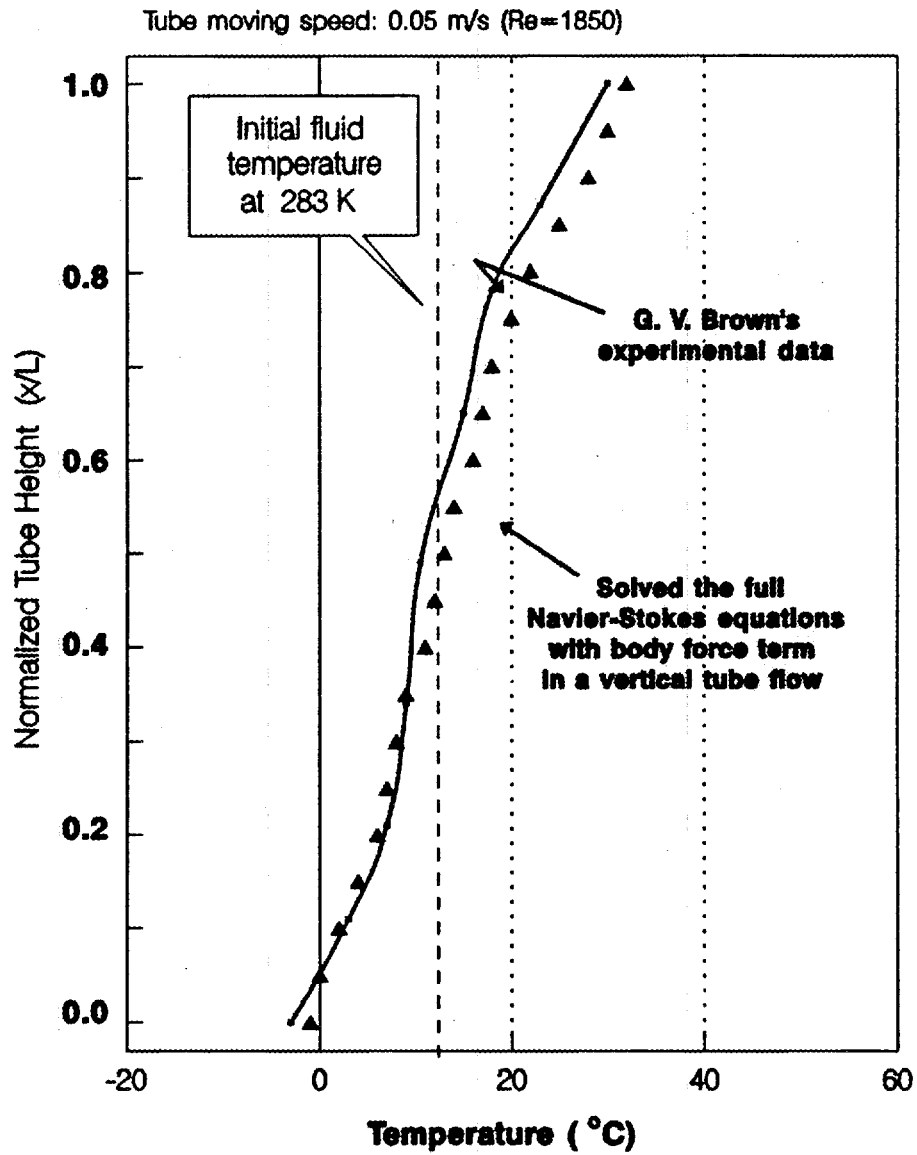


Fig. 3.2 Physical model of the regenerator tube in a magnetic heat pump with no heat exchangers present.

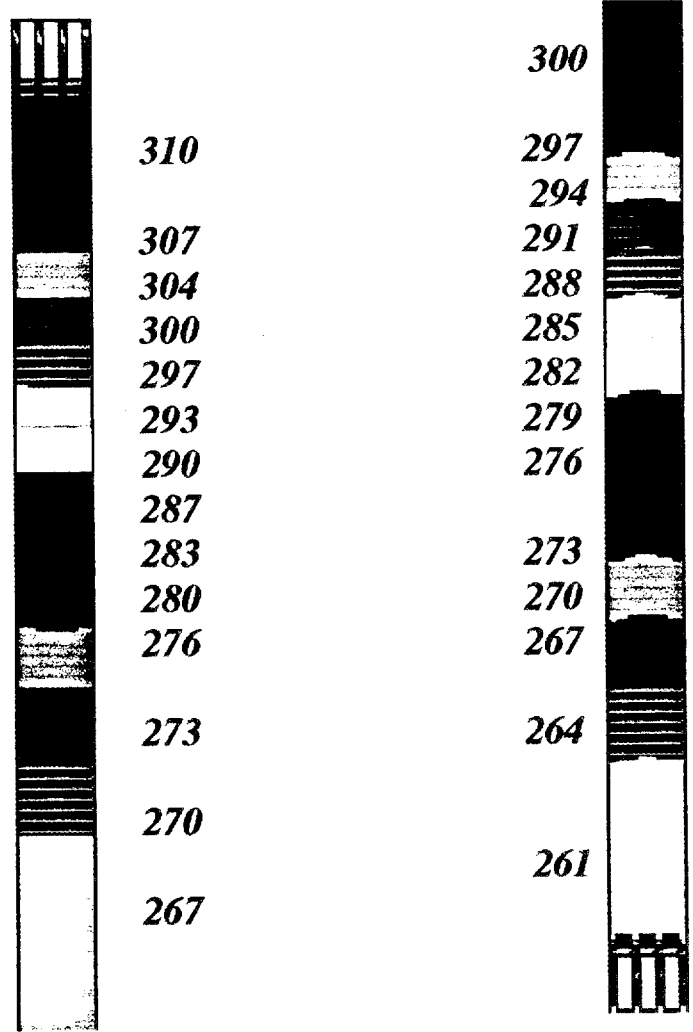


**Fig. 3.3. Gadolinium adiabatic temperature lift for 7 Tesla from molecular field theory.**



**Fig. 3.4.** Temperature distribution in the regenerator fluid column after 10 cycles (validation of the computer code).

*Temperature (K)*



*(A) Magnetization  
(t=1398 s, 19.5 cycles)*

*(B) Demagnetization  
(t=1434 s, 20 cycles)*

**Fig. 3.5. Temperature color rasters in the regenerator fluid column with no heat exchangers present (Re=1630).**

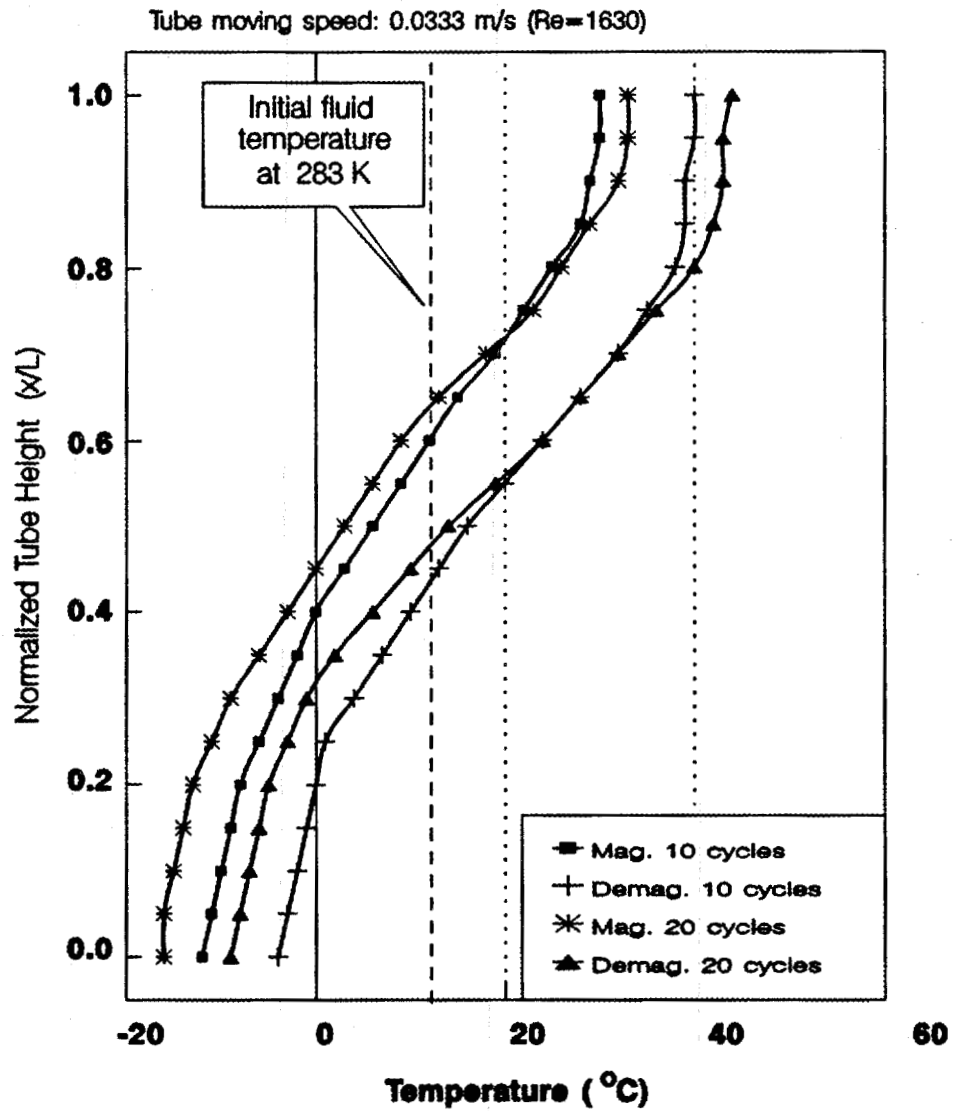


**Fig. 3.6.** Development of temperature distribution in the regenerator fluid column with no heat exchangers present ( $Re=1630$ ).

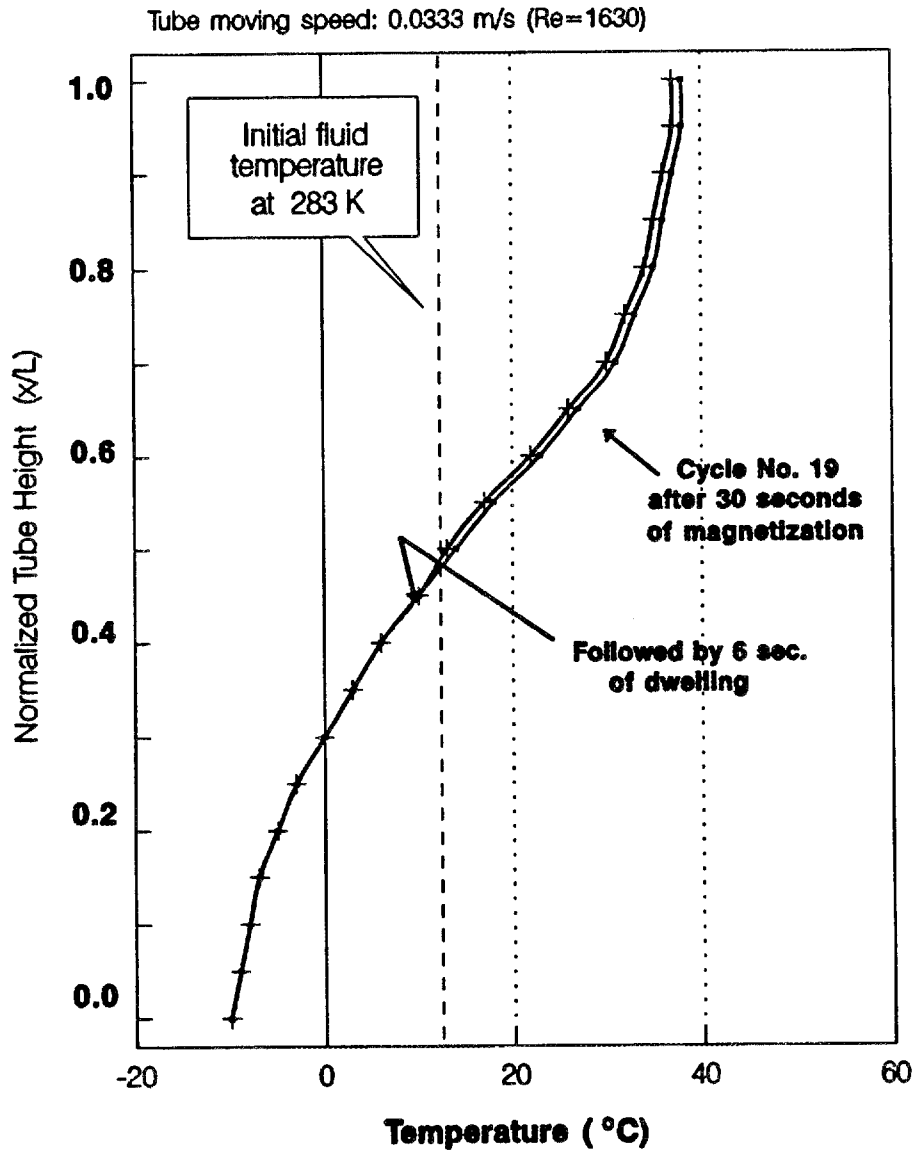
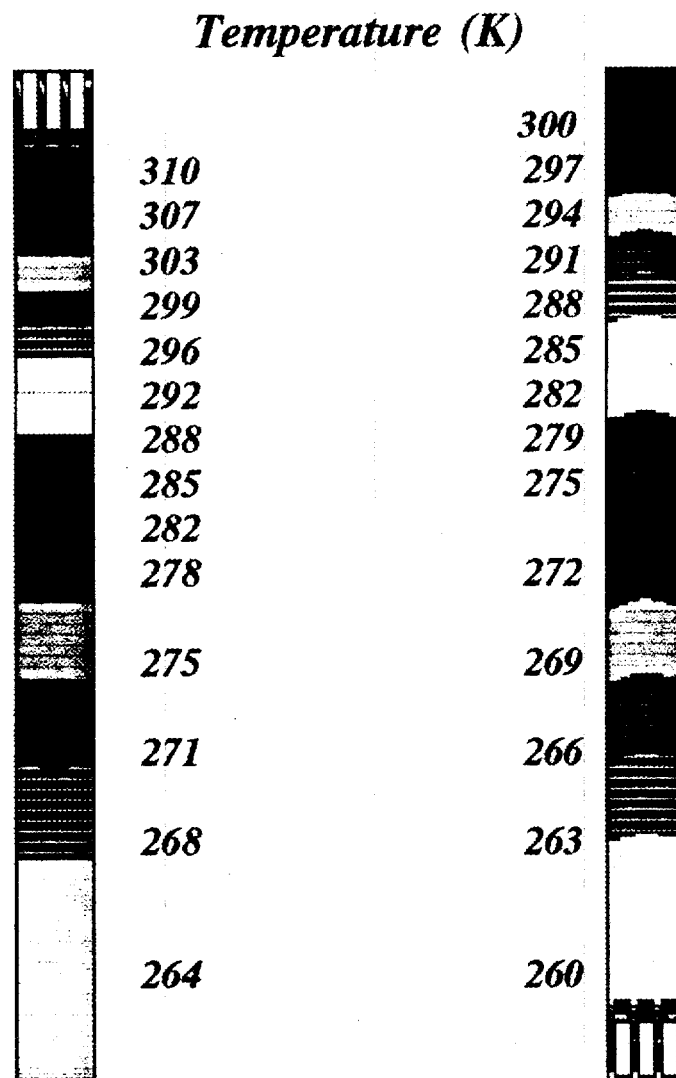


Fig. 3.7. Comparison of temperature distribution in the regenerator fluid column before and after dwelling.



*(A) Magnetization  
(t=1282 s, 11.5 cycles)*

*(B) Demagnetization  
(t=1338 s, 12 cycles)*

**Fig. 3.8. Temperature color rasters in the regenerator fluid column with no heat exchangers present (Re=980).**

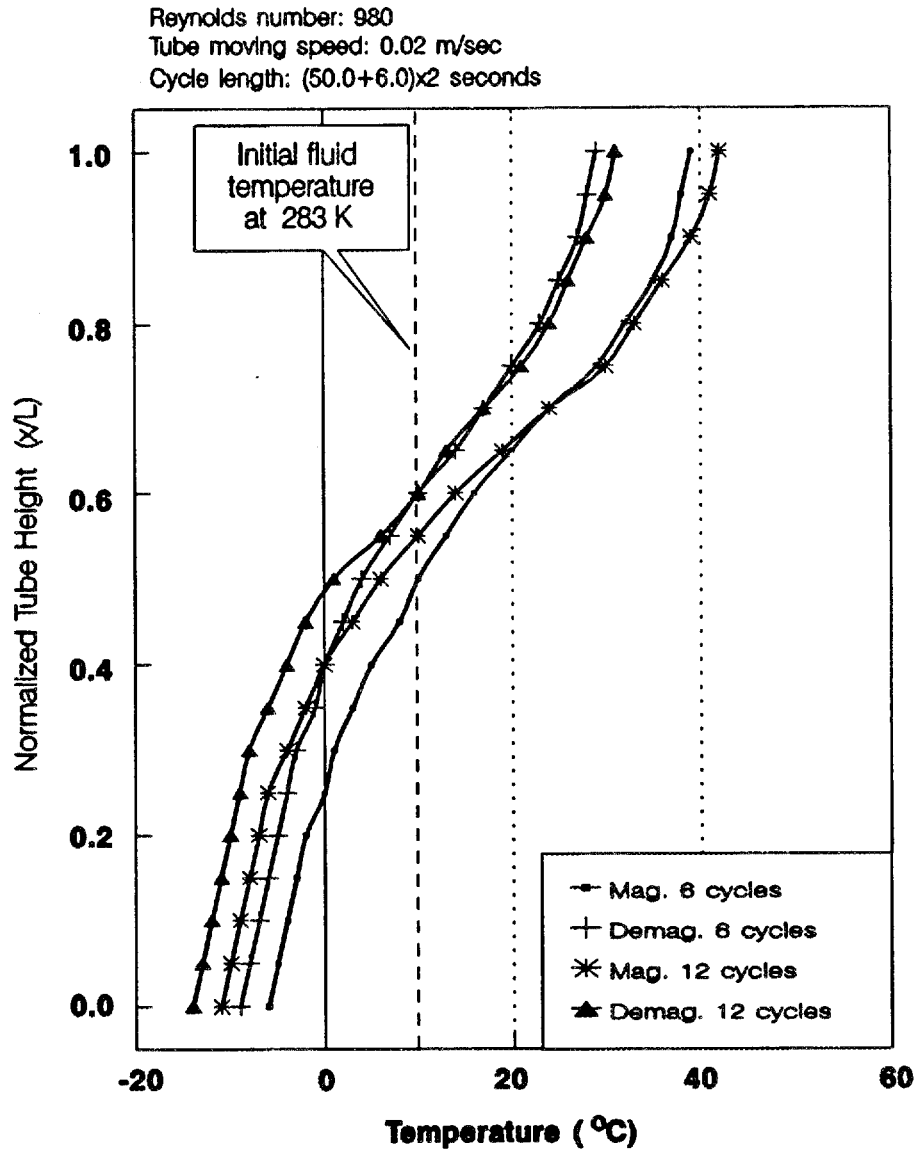
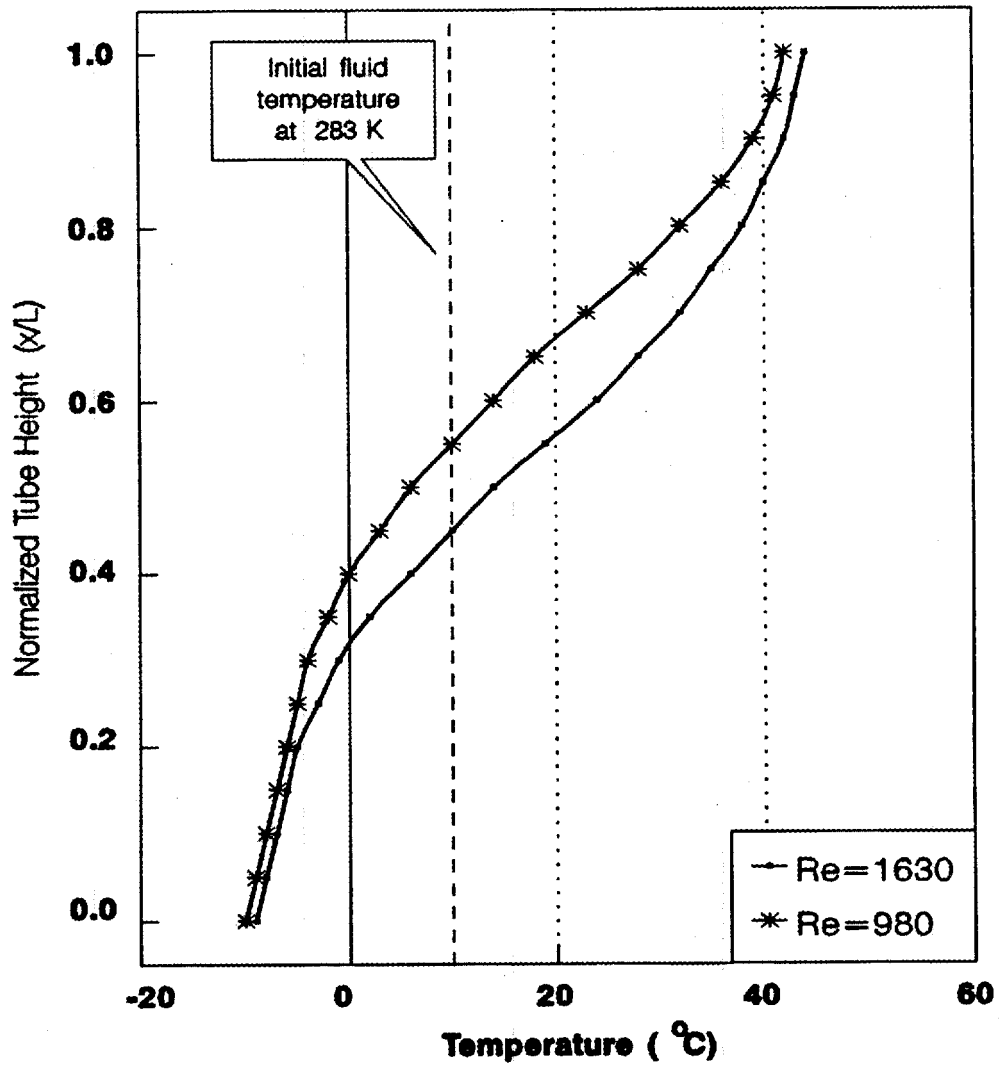


Fig. 3.9. Development of temperature distribution in the regenerator fluid column with no heat exchangers present ( $Re=980$ ).



**Fig. 3.10.** Comparison of the temperature distribution in the regenerator fluid column with no heat exchangers present for two flow cases,  $Re=1630$  and  $Re=980$ .

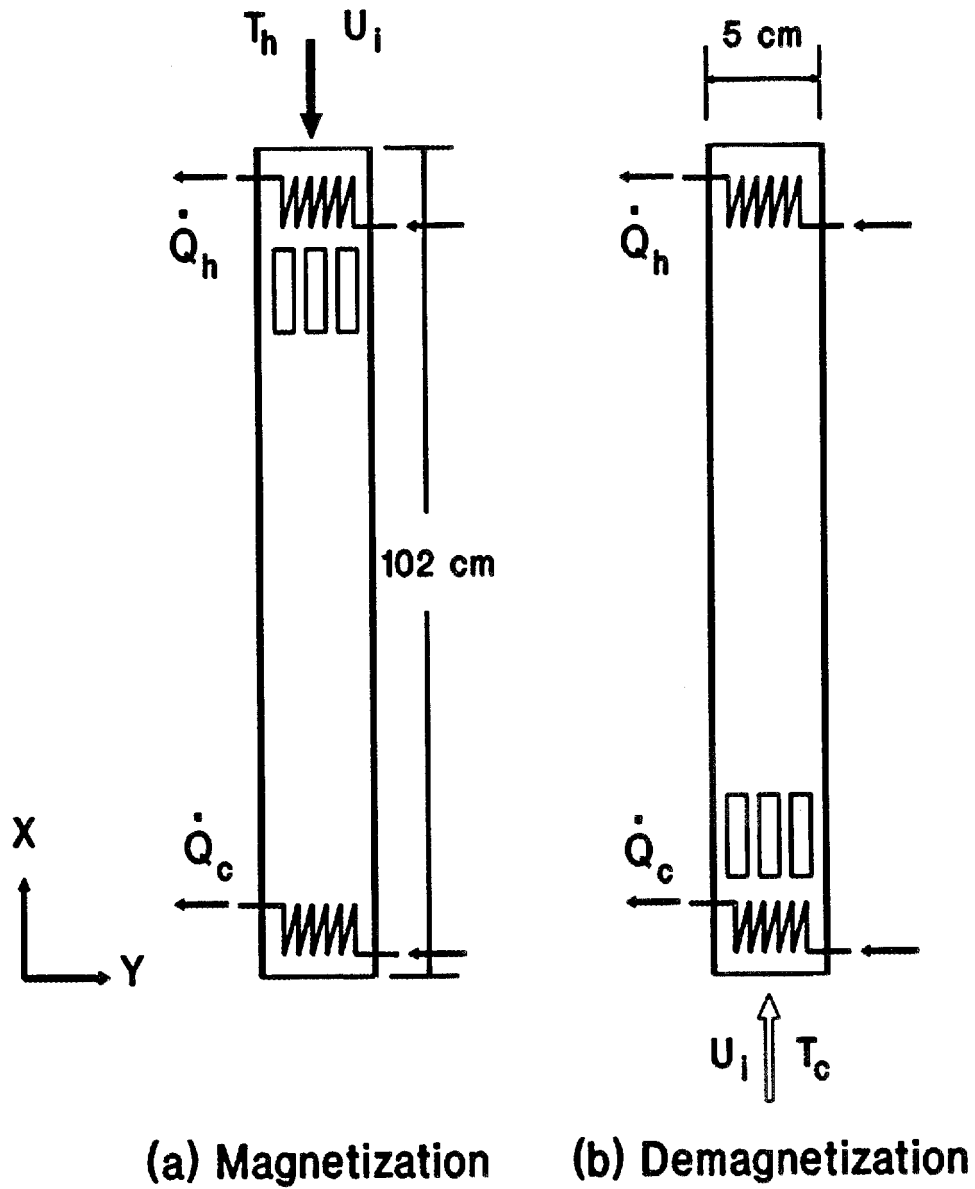
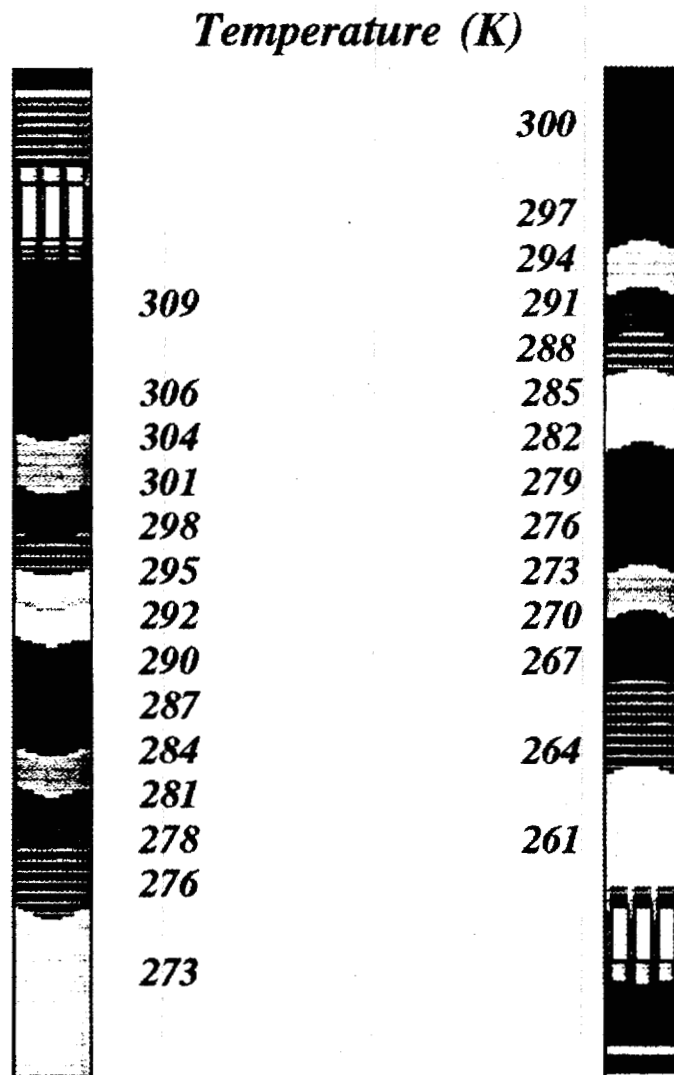


Fig. 3.11. Physical model of the regenerator tube in a magnetic heat pump with heat exchangers present.



**(A) Magnetization**  
*(t=1150 s, 11.5 cycles)*

**(B) Demagnetization**  
*(t=1200 s, 12 cycles)*

**Fig. 3.12.** Temperature color rasters in the regenerator fluid column with heat exchangers present ( $Re=980$ ).

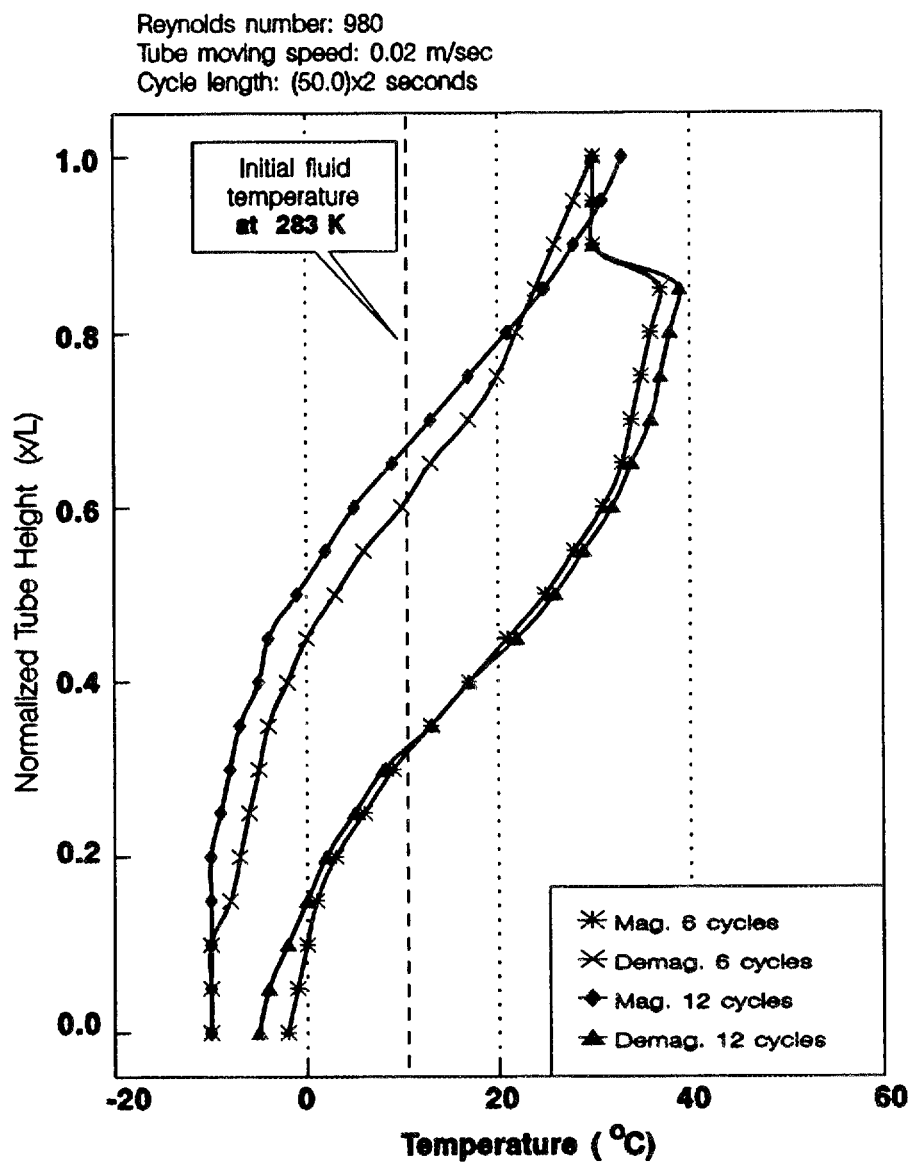
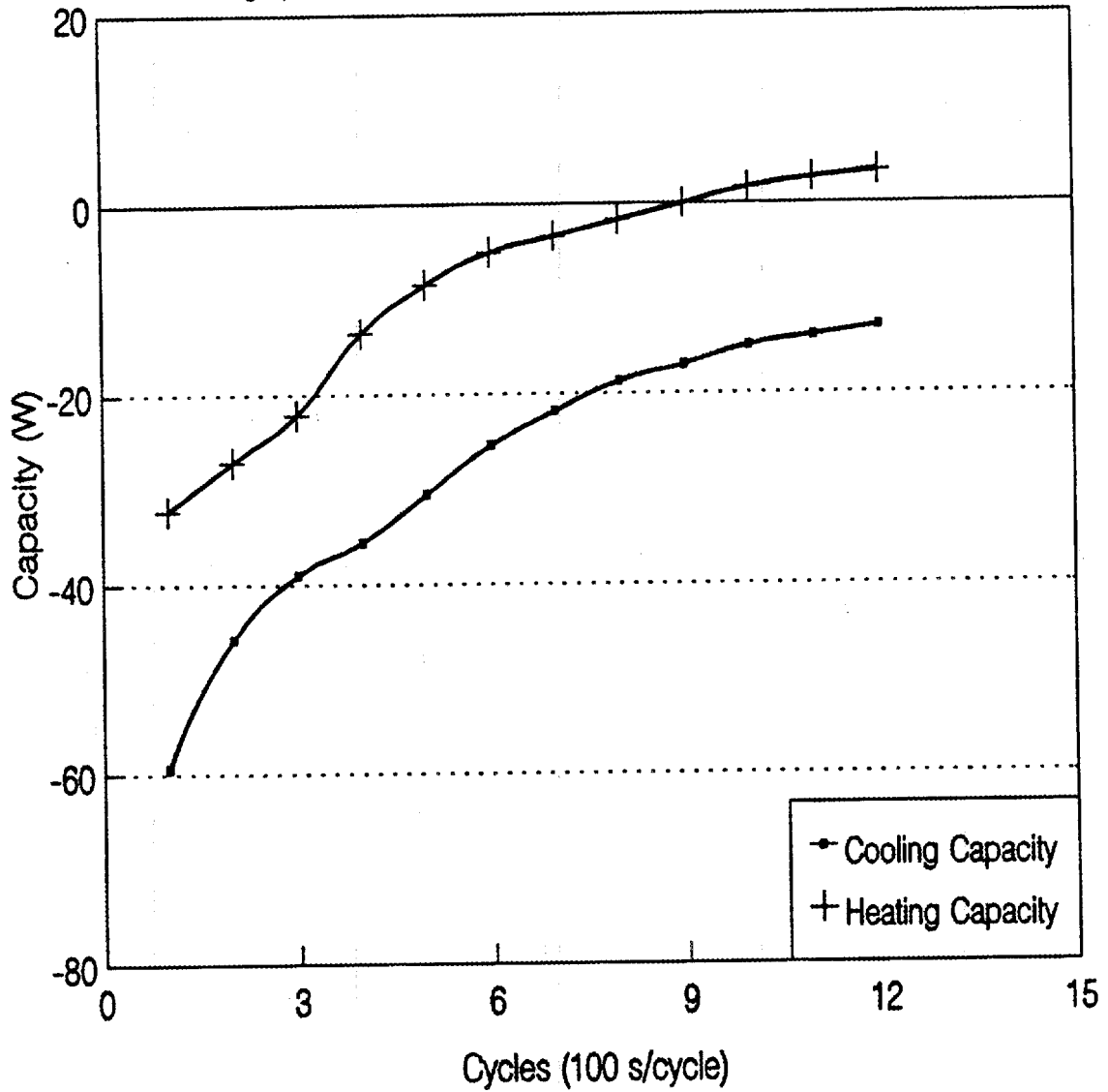
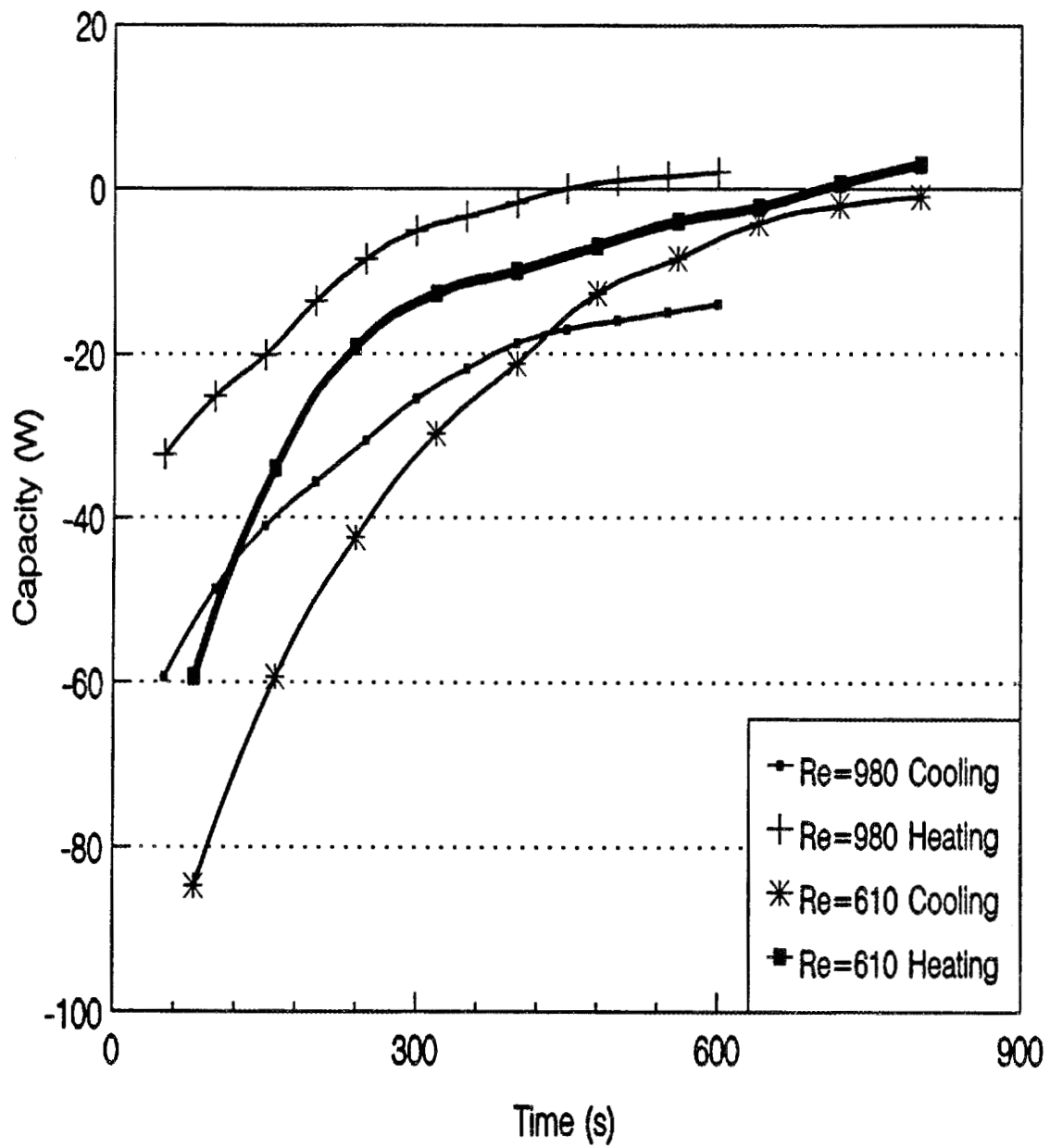


Fig. 3.13. Development of temperature distribution in the regenerator fluid column with heat exchangers present ( $Re=980$ , after 12 cycles).

Reynolds number: 980  
50% Methanol + 50% Water  
Tube moving speed: 0.02 m/sec



**Fig. 3.14.** Energy delivery rates from and to the hot and cold reservoirs after 12 cycles in the case of  $Re=980$ .



**Fig. 3.15. Comparison of energy delivery rates as the function of charge time for flow rate cases of Re=980 and Re=610.**

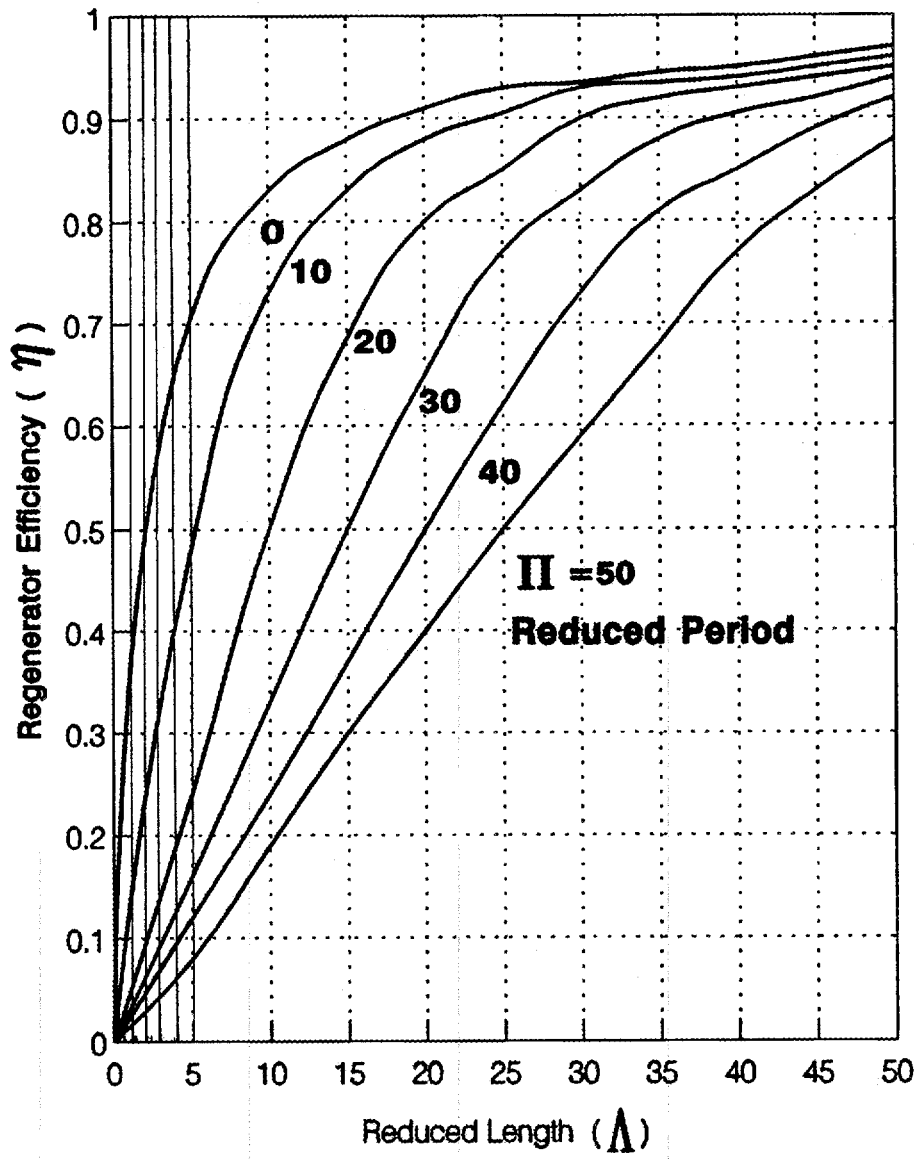


Fig. 3.16. Regenerator efficiency as a function of reduced length and reduced period (From ref. 27).



**Fig. 4.1. Overview of the gadolinium core.**

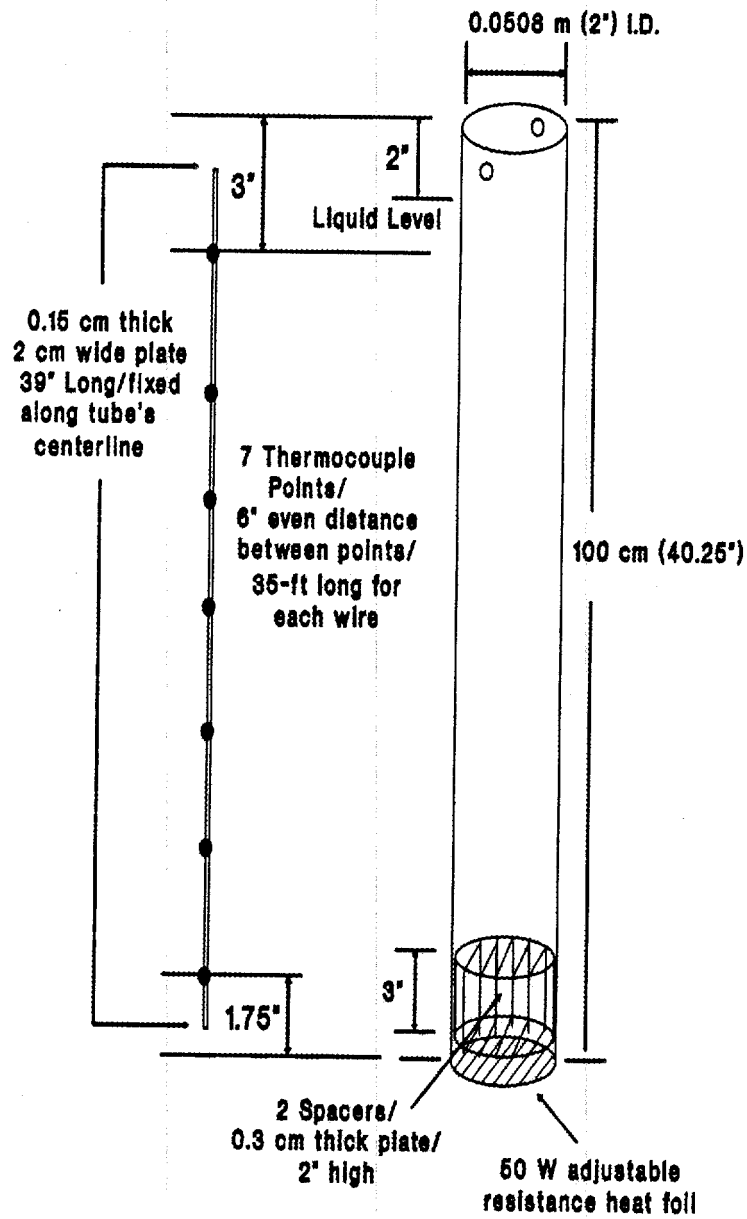
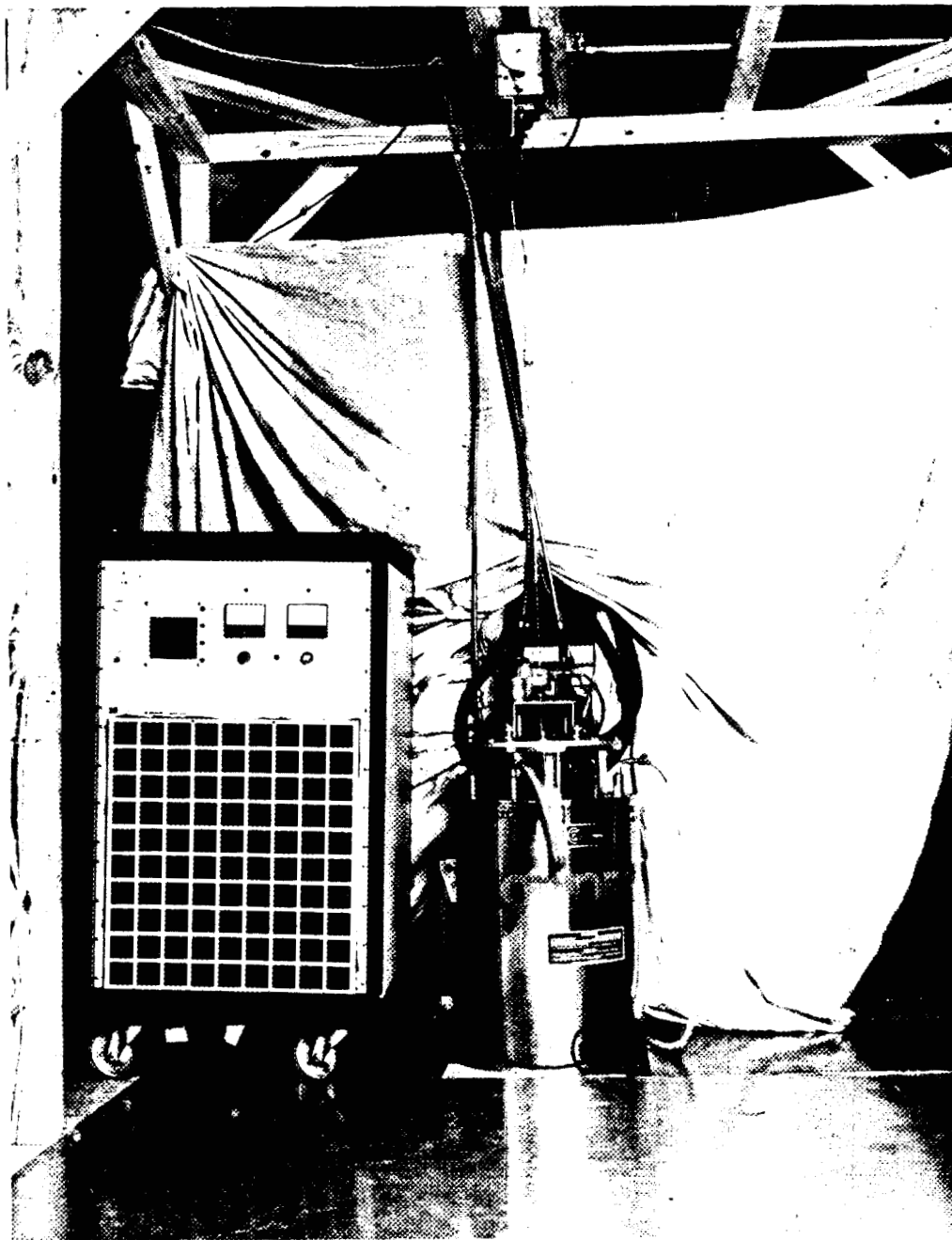


Fig. 4.2. A thermocouples column in the regenerator tube.



**Fig. 4.3. Overview of the reciprocating magnetic heat pump test setup.**

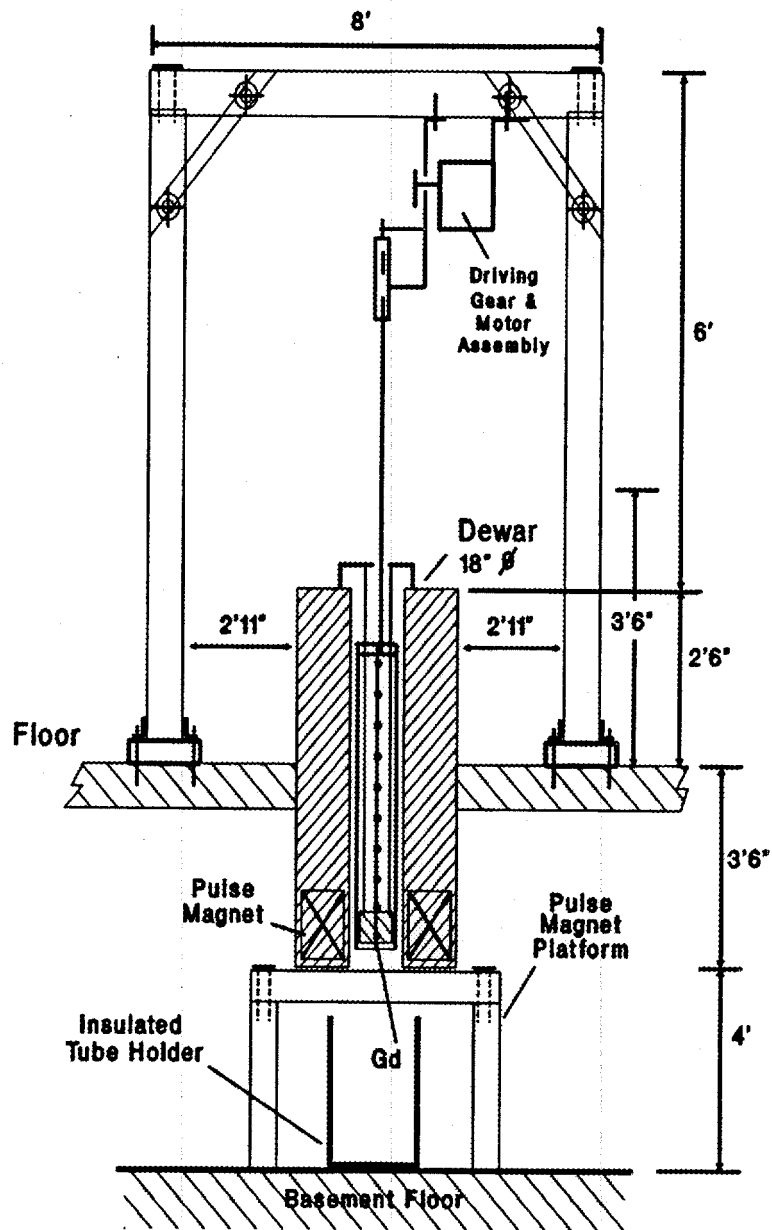
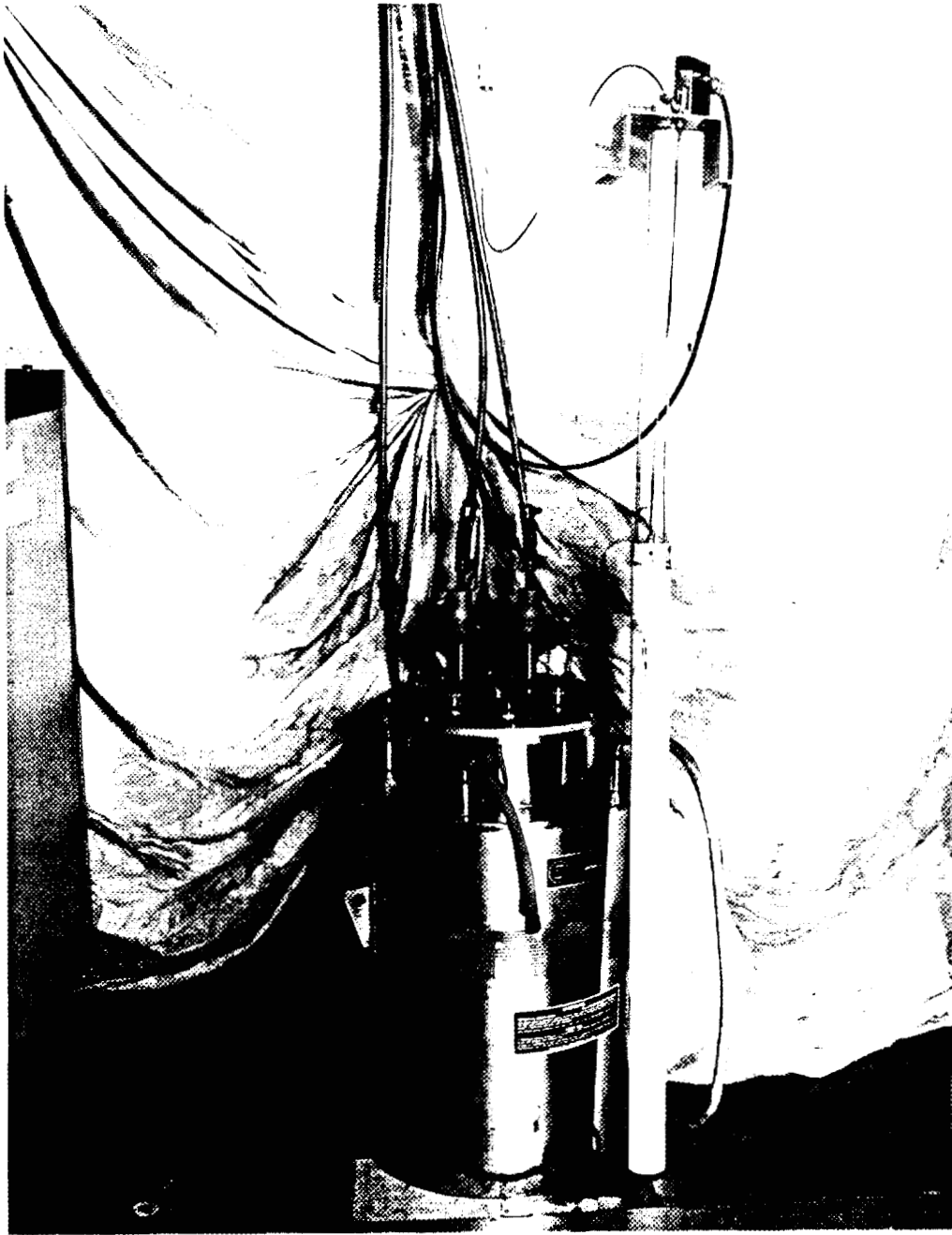


Fig. 4.4. Schematic of the reciprocating magnetic heat pump test setup.



**Fig. 4.5. Overview of the regenerator tube with gadolinium core inside.**

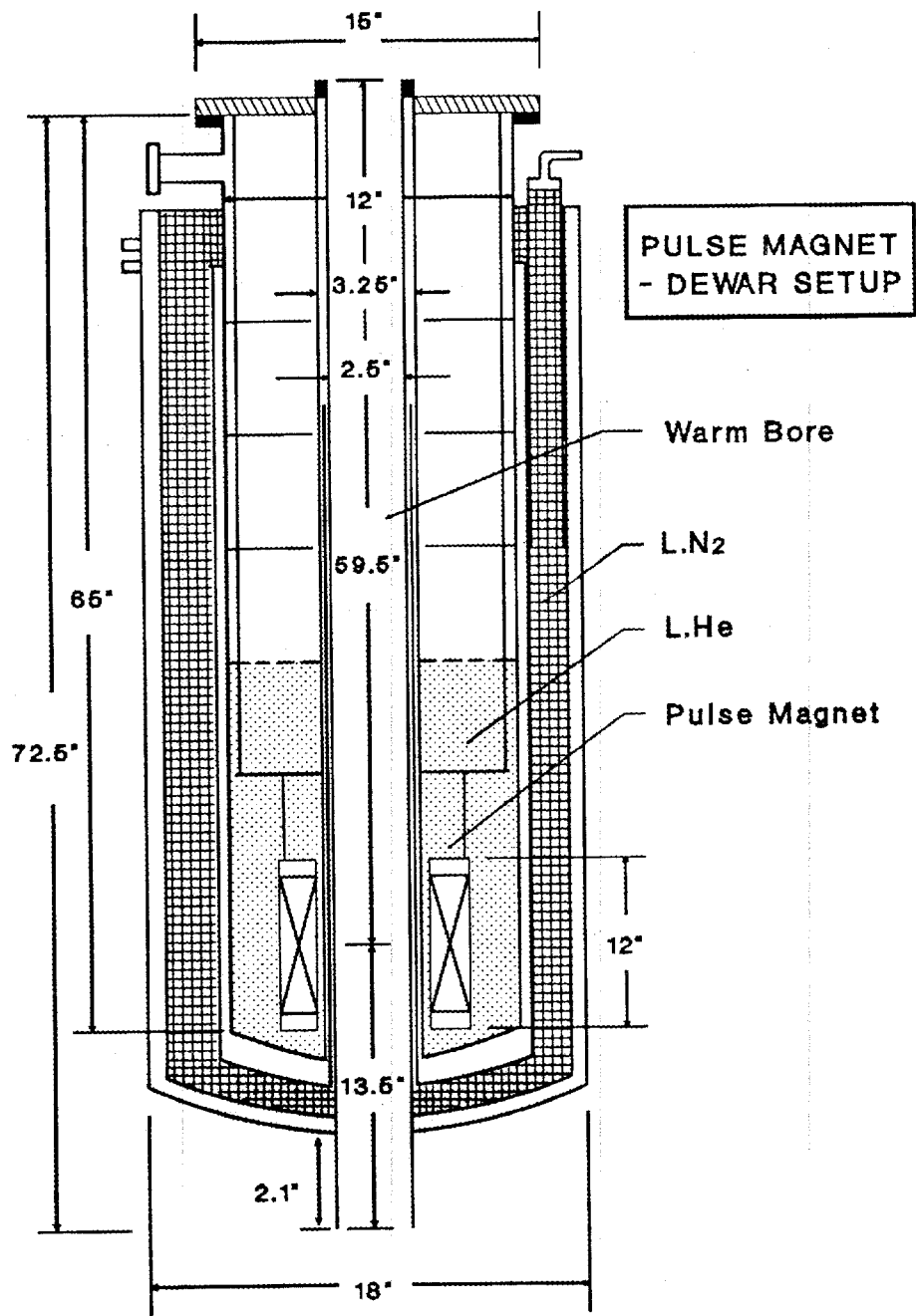


Fig. 4.6. Schematic of the superconducting pulse magnet dewar.

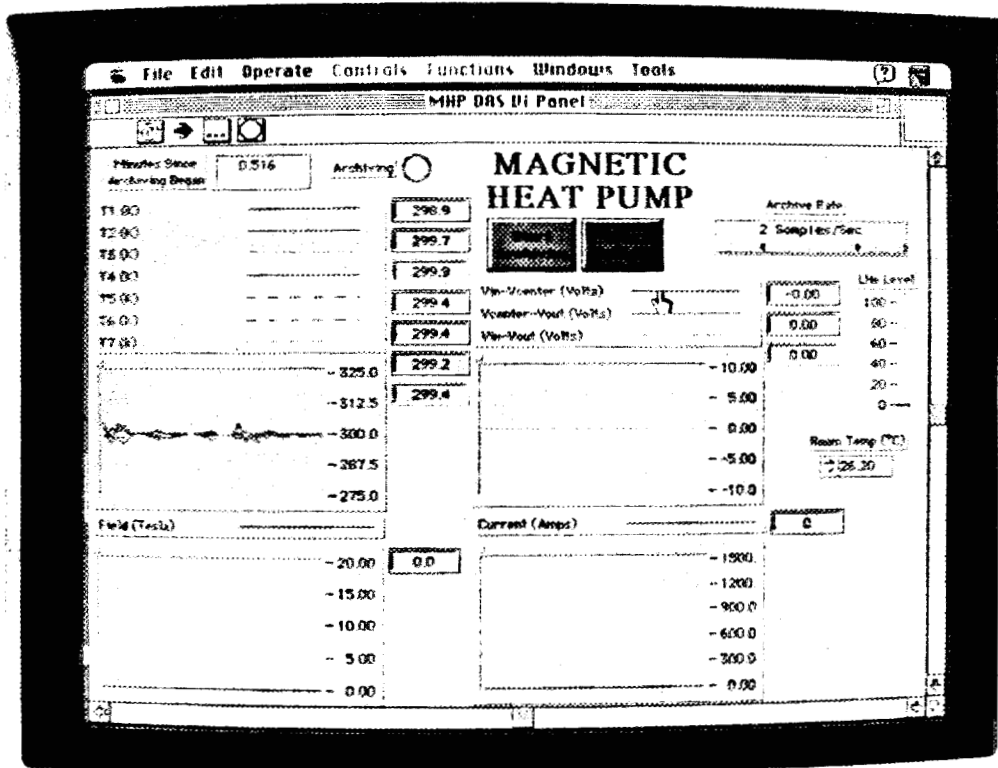
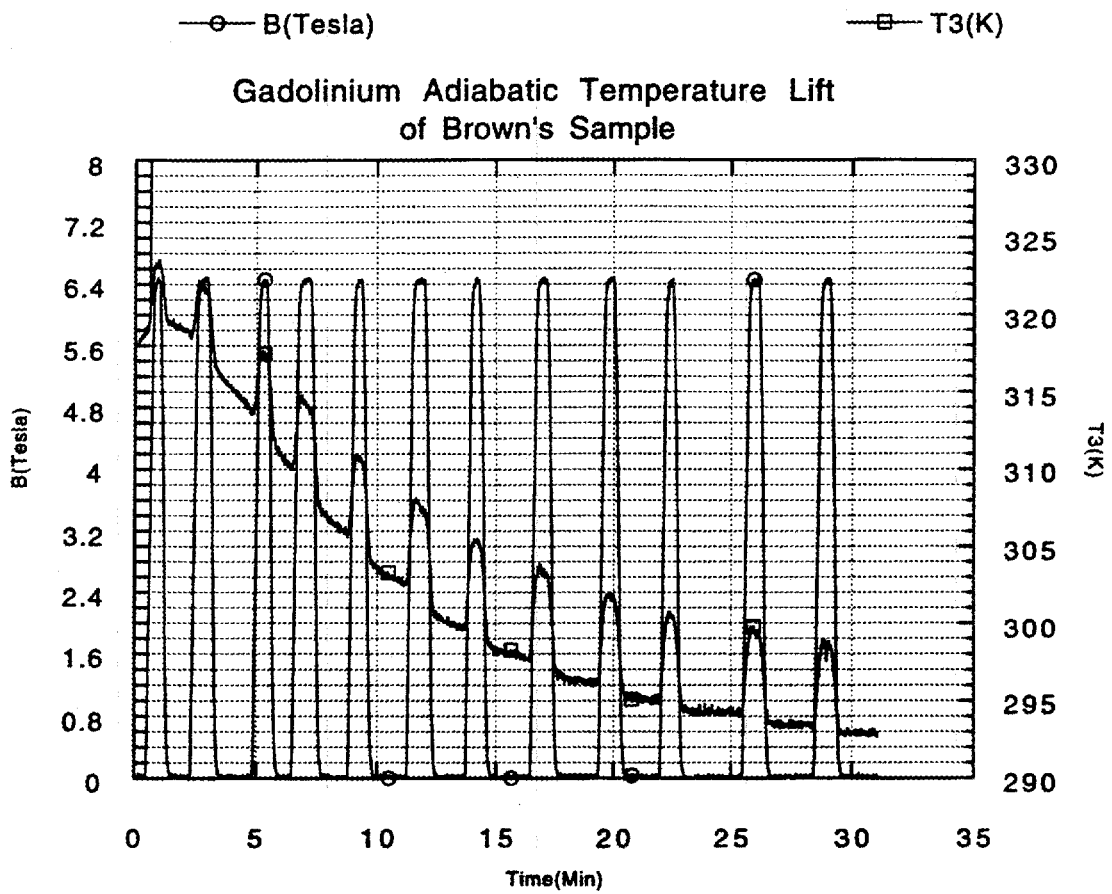
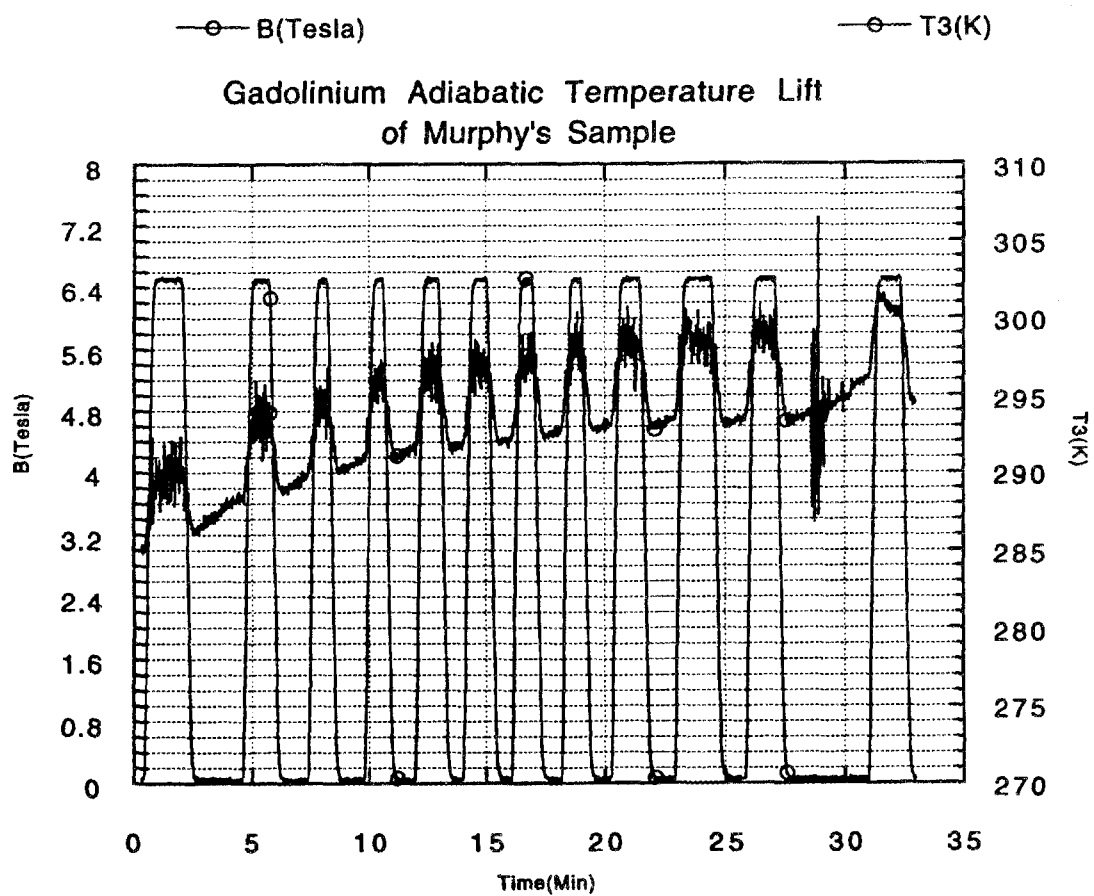


Fig. 4.7. LabView IV for system monitoring and control.



**Fig. 4.8. Measurement of gadolinium adiabatic temperature lift of Brown's sample.**



**Fig. 4.9. Measurement of gadolinium temperature lift  
of ORNL's sample.**

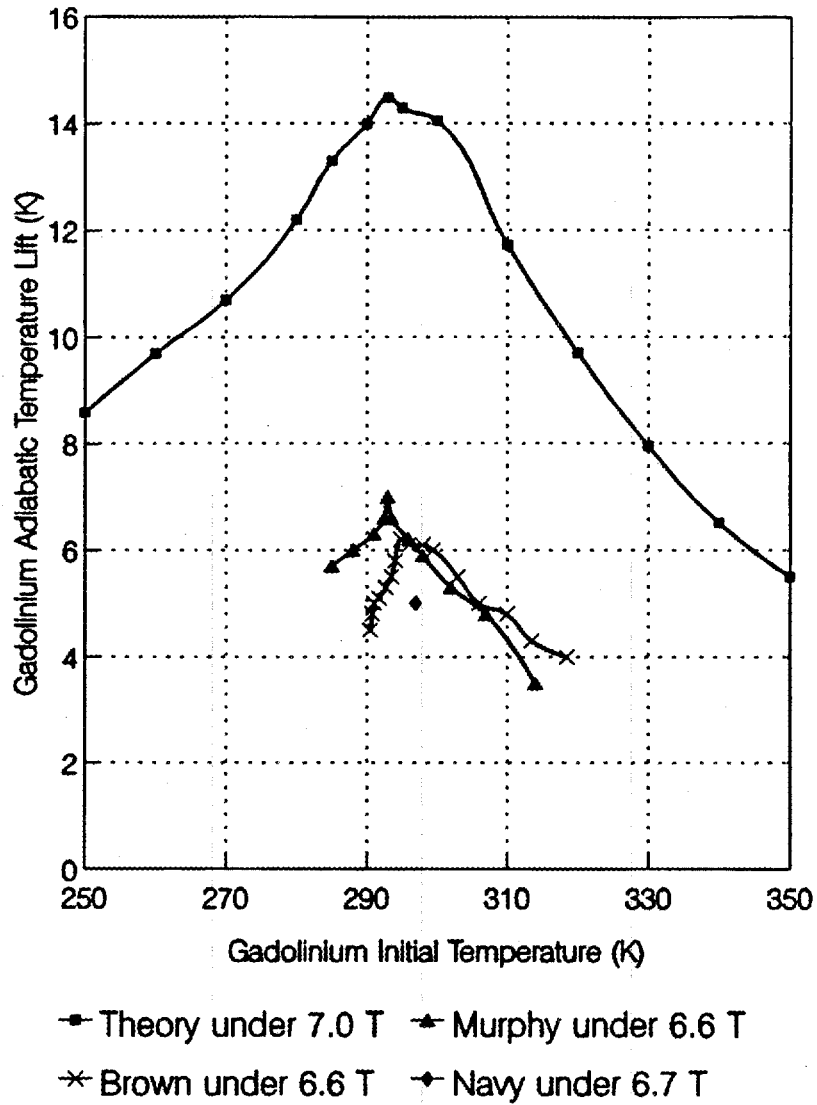
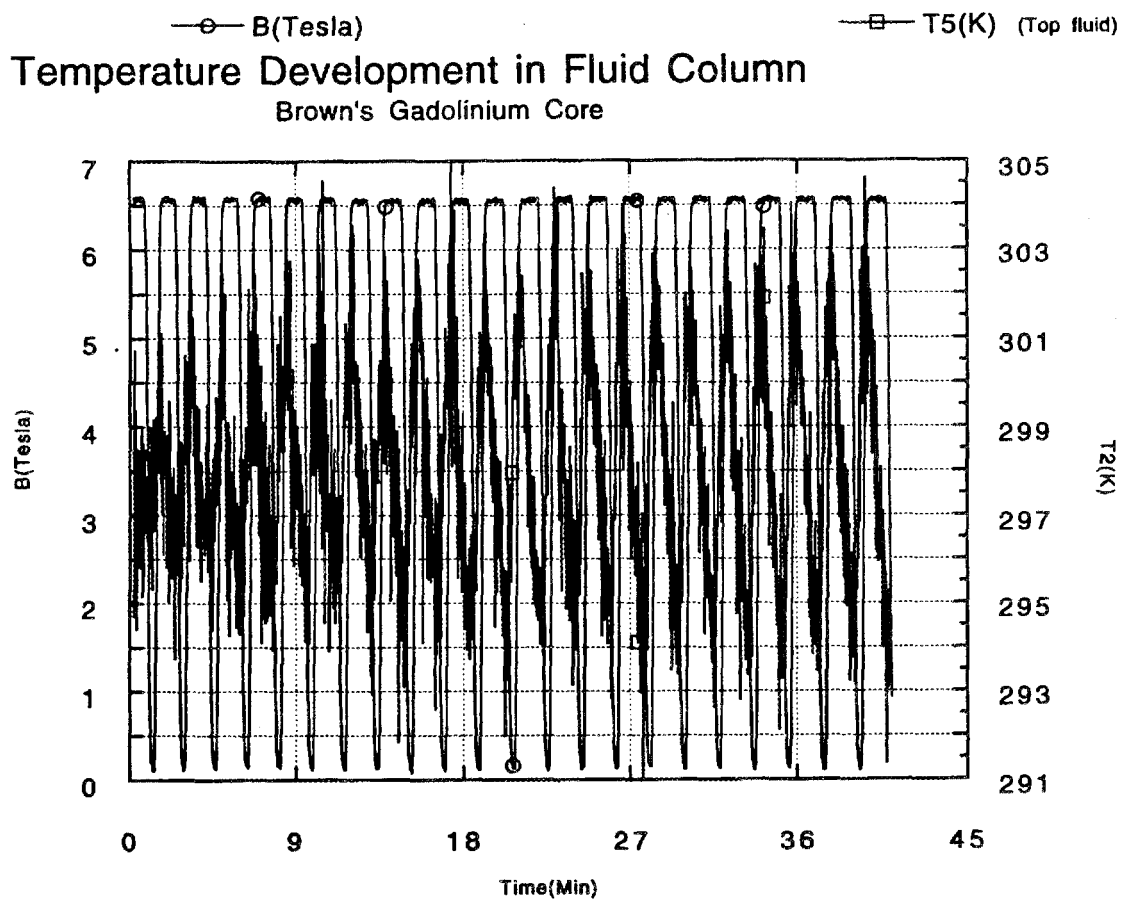
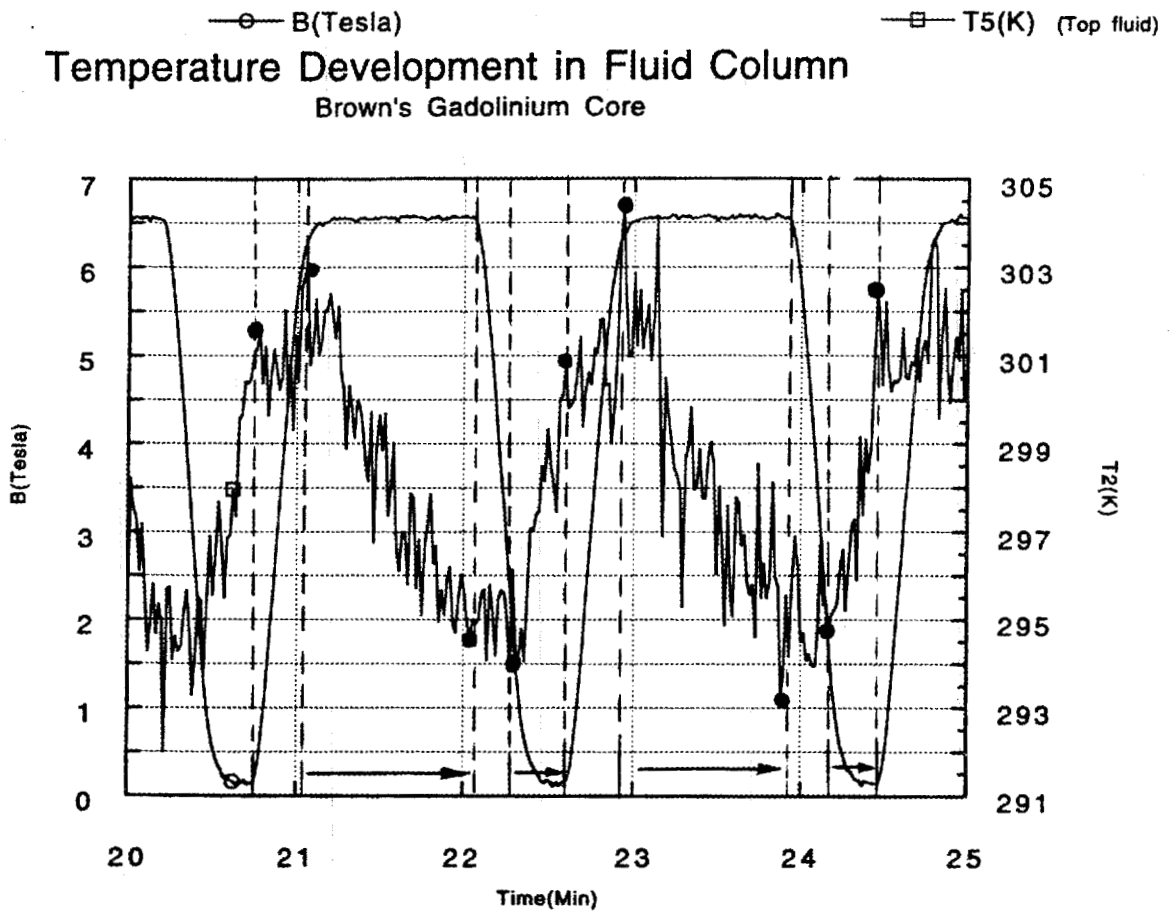


Fig. 4.10. Comparison of gadolinium temperature lift among samples.



**Fig. 4.11. Temperature development in the regenerator fluid column for the case of average  $Re=300$ .**



**Fig. 4.12.** Temperature development along with the magnetic heat pumping process at average  $Re=300$ .

Reynolds number: 300  
Tube moving speed: 0.90 m/37 sec  
Cycle length: (15.0+37.0)x2 seconds  
Based on 6 K of Gd (at 293 K) adiabatic temp. lift

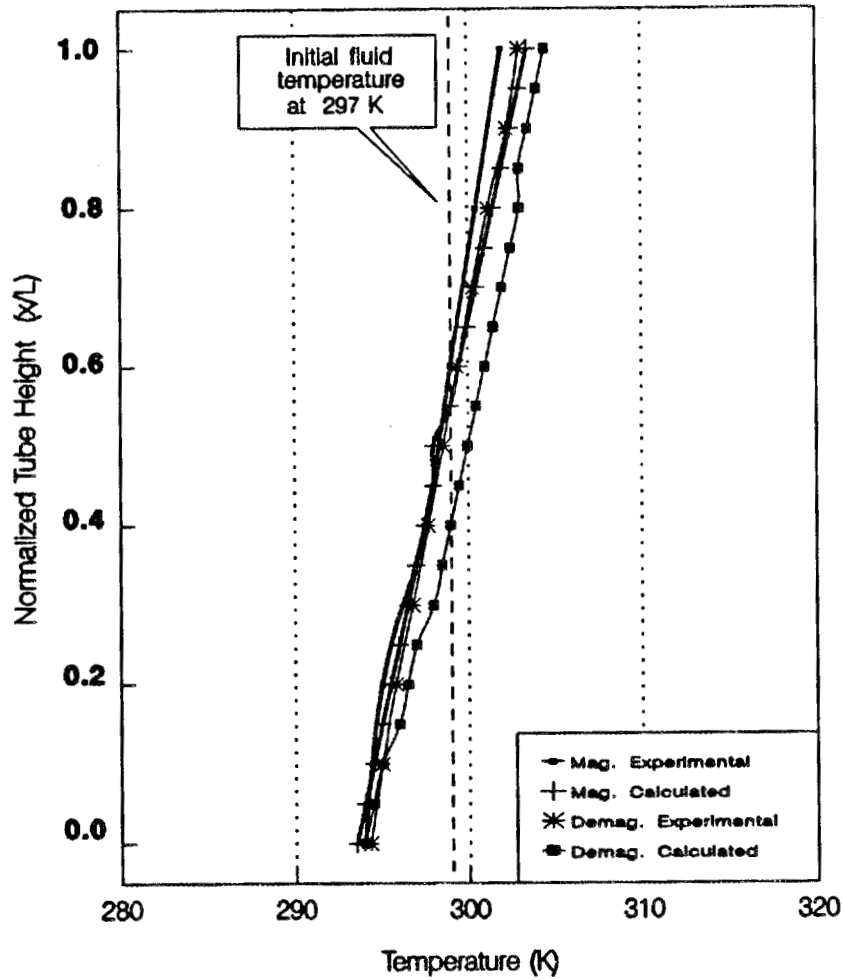


Fig. 4.13. Comparison of temperature development in the regenerator fluid column between experimental data and calculated values.

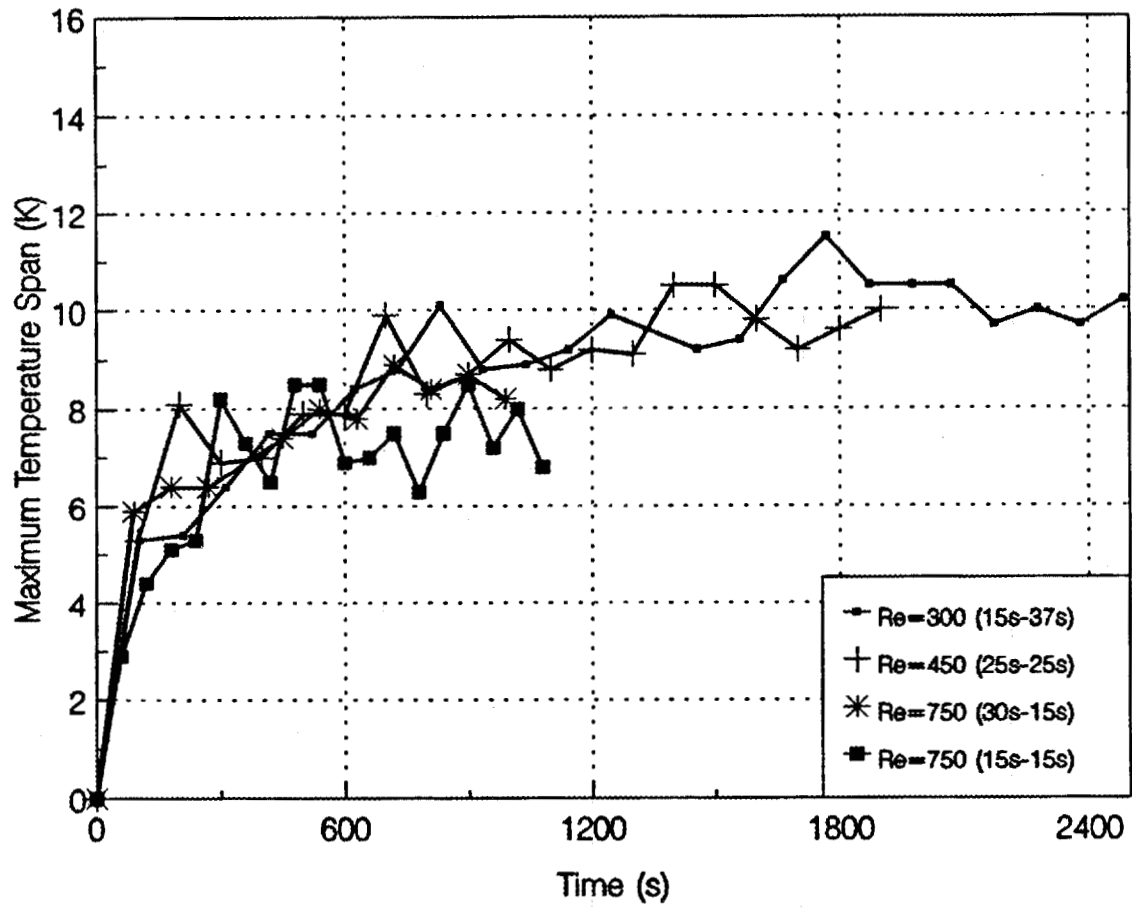
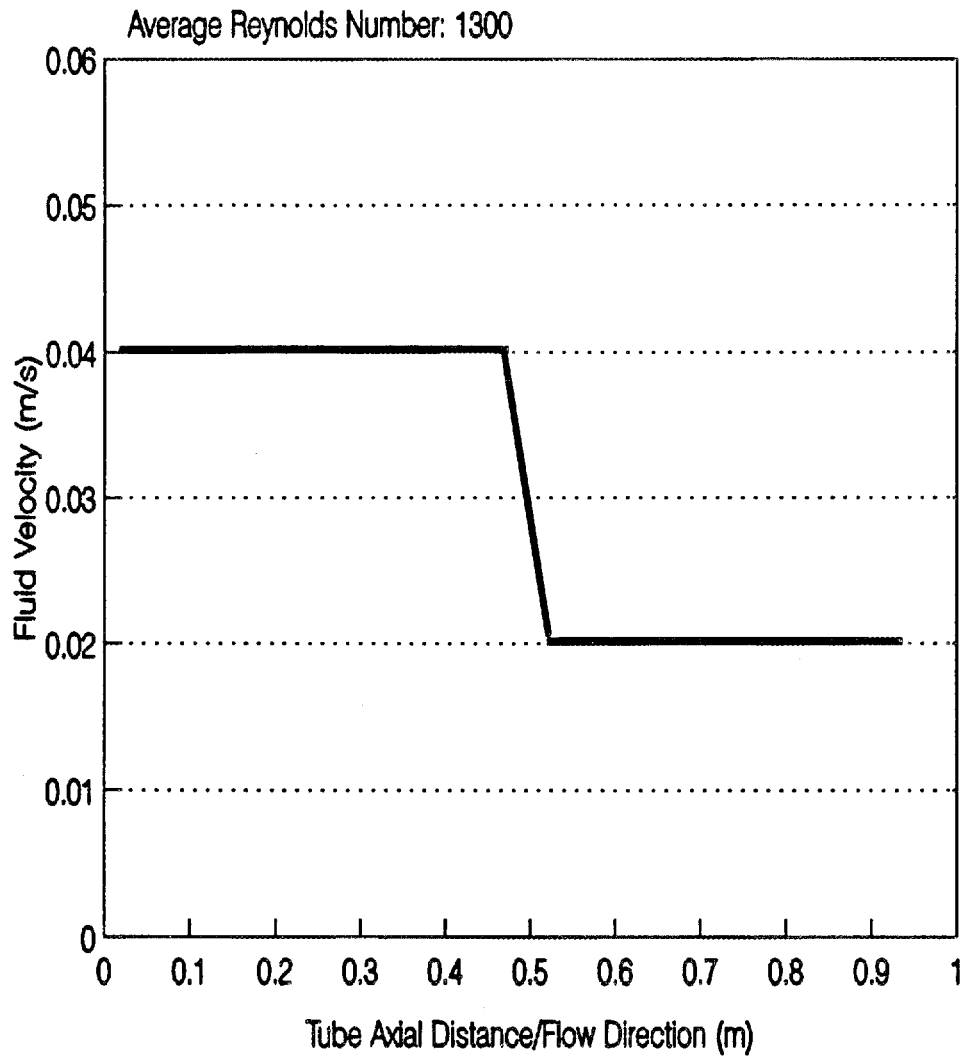


Fig. 4.14. Comparison of maximum temperature spans among cases with different Reynolds number.



**Fig. 4.15. Stepwise variation of velocity in the flow direction.**

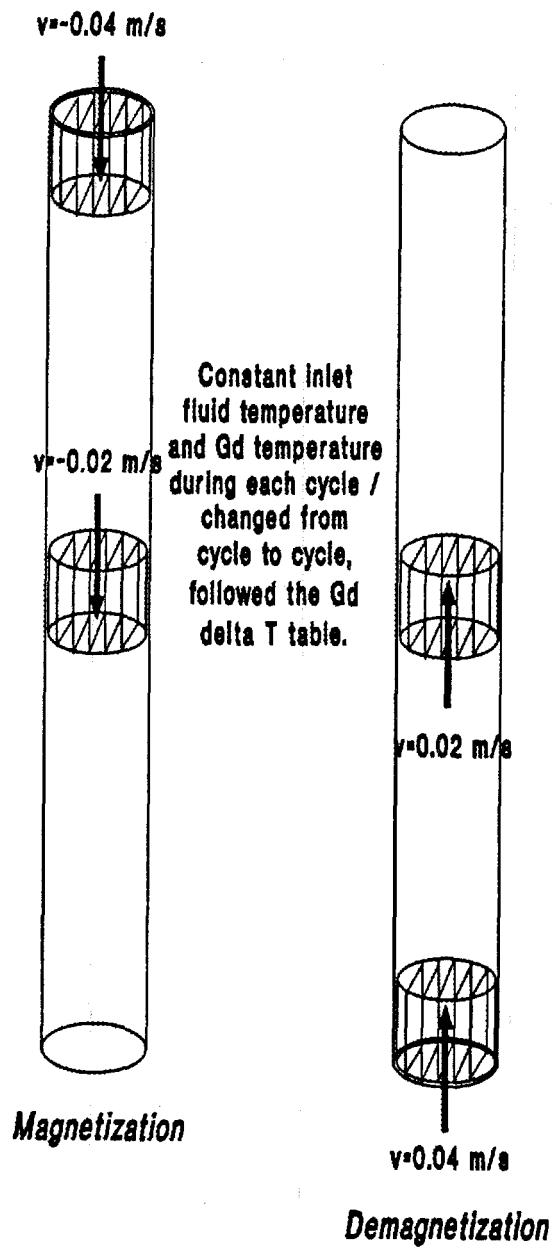


Fig. 4.16. Two-speed transient regenerator tube flow of room temperature magnetic heat pumps.

Average Reynolds number: 1300  
Tube moving speed: 0.45/22.5, 0.45/11.25 (m/sec)  
Two stage: (22.5+11.25)x2 seconds

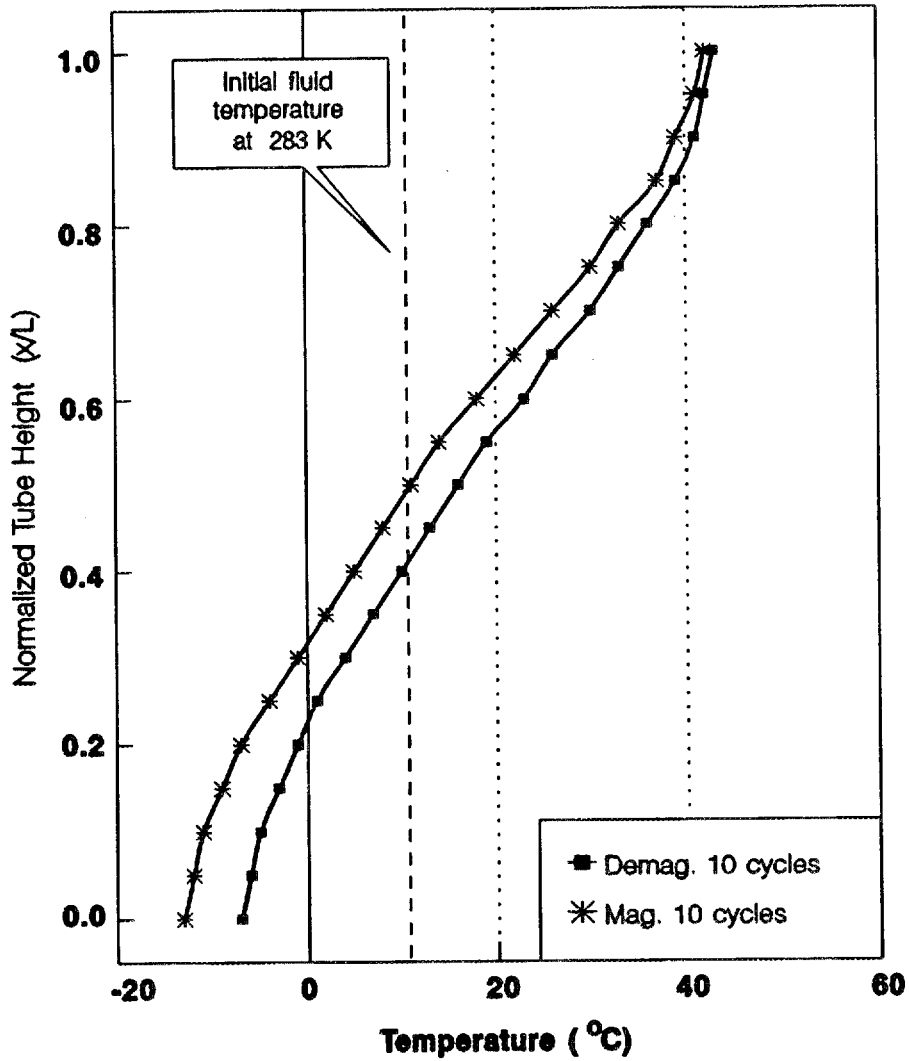


Fig. 4.17. Temperature distribution in the regenerator fluid column using stepwise tube moving speeds of 0.04 and 0.02 m/sec.

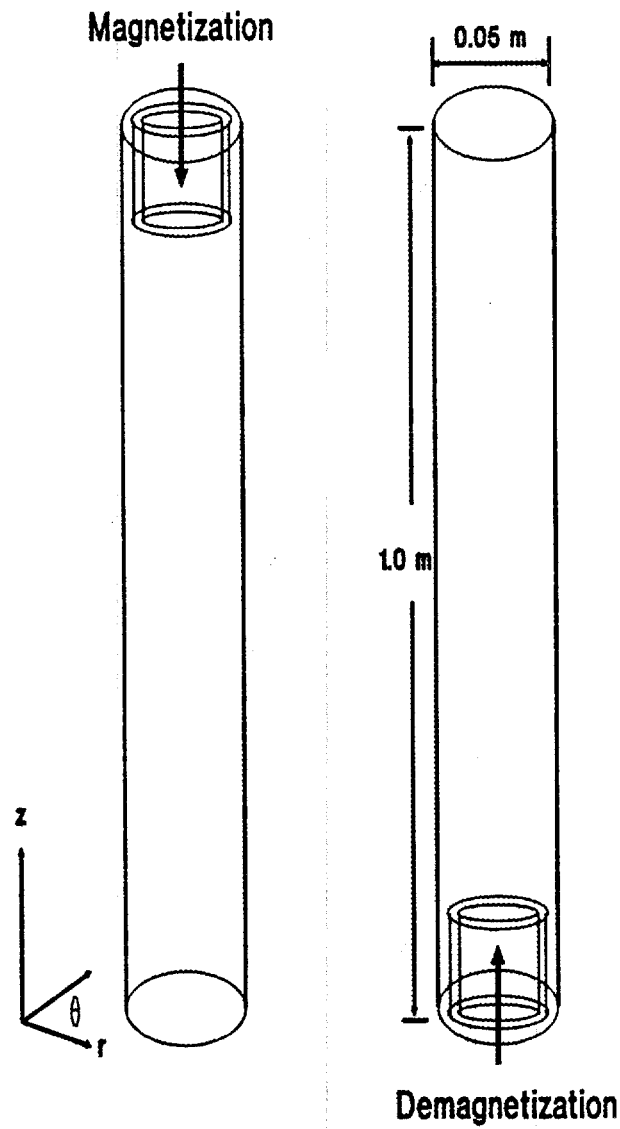
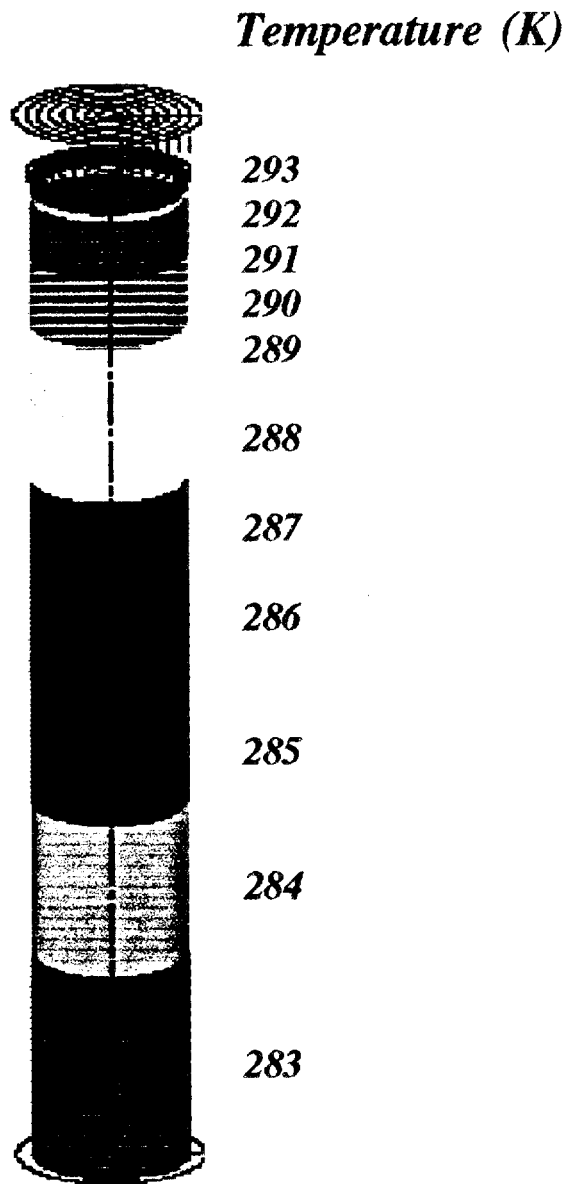


Fig. 4.18. Three-dimensional geometry of flow problem.



**Fig. 4.19.** Temperature color raster in a three-dimensional regenerator fluid column.

**Appendix A:**

**The combined natural and forced convection in the  
regenerator tube flow of magnetic heat pumps**

**The combined natural and forced convection in the regeneration tube flow of magnetic heat pumps**

The criterion for judging the heat transfer mechanism in the regenerator tube flow of the magnetic heat pumps is as follows (for fluids  $Pr > 1$ ):

$$\frac{Ra^{\frac{1}{4}}}{Re^{\frac{1}{2}} Pr^{\frac{1}{3}}} > O(1), \quad \text{Natural Convection ;} \quad (A1)$$

$$\frac{Ra^{\frac{1}{4}}}{Re^{\frac{1}{2}} Pr^{\frac{1}{3}}} < O(1), \quad \text{Forced Convection .} \quad (A2)$$

where,  $Ra$  and  $Pr$  are the Rayleigh number and Prandtl number of the fluid.

For the 50% ethylene glycol and 50% water working fluid, it is assumed that the Prandtl number is about 10 in a moderate temperature; and the highest Reynolds number is expected to be no more than 2300 in our experiment. Thus, we can calculate the ratio indicated in Eqs. (1) and (2) with the following definitions and data:

$$Ra = Gr.Pr = \frac{g.\beta.(\Delta T).H^3}{\nu^2}.Pr = \frac{(9.8).\left(\frac{1}{300}\right).(4).(0.1)^3}{(4.0 \times 10^{-6})^2} \cdot (10) \approx 8.167 \times 10^7. \quad (A3)$$

where,  $Gr$  is the Grashof number of the fluid.

Therefore,

$$\frac{Ra^{\frac{1}{4}}}{Re^{\frac{1}{2}}Pr^{\frac{1}{3}}} = \frac{(8.167 \times 10^7)^{\frac{1}{4}}}{(1500)^{\frac{1}{2}} \cdot (10)^{\frac{1}{3}}} = 1.140 \approx 1.0 \quad (\text{A4})$$

Based on this calculation for a typical case in the regenerator tube flow, with Rayleigh number,  $Ra=8.167 \times 10^7$ , the flow is already in the turbulent natural convection regime. However, in a moderately high Reynolds number case of  $Re=1500$ , the ratio (it is actually a ratio between natural convection and forced convection) in Eqs. (1) and (2) is on the order of 1. Thus, we can conclude that the heat transfer mechanism in the fluid column of the regenerator tube flow for a typical operating case is a combination of natural and forced convection. They co-exist in about the same order of magnitude in most of the cases. Therefore, although the Reynolds number is an appropriate parameter for describing the characteristics of the regenerator tube flow of MHPs, we certainly cannot neglect the buoyancy force term in solving for regenerator tube flow.

**Appendix B:**

**Experimental Data**

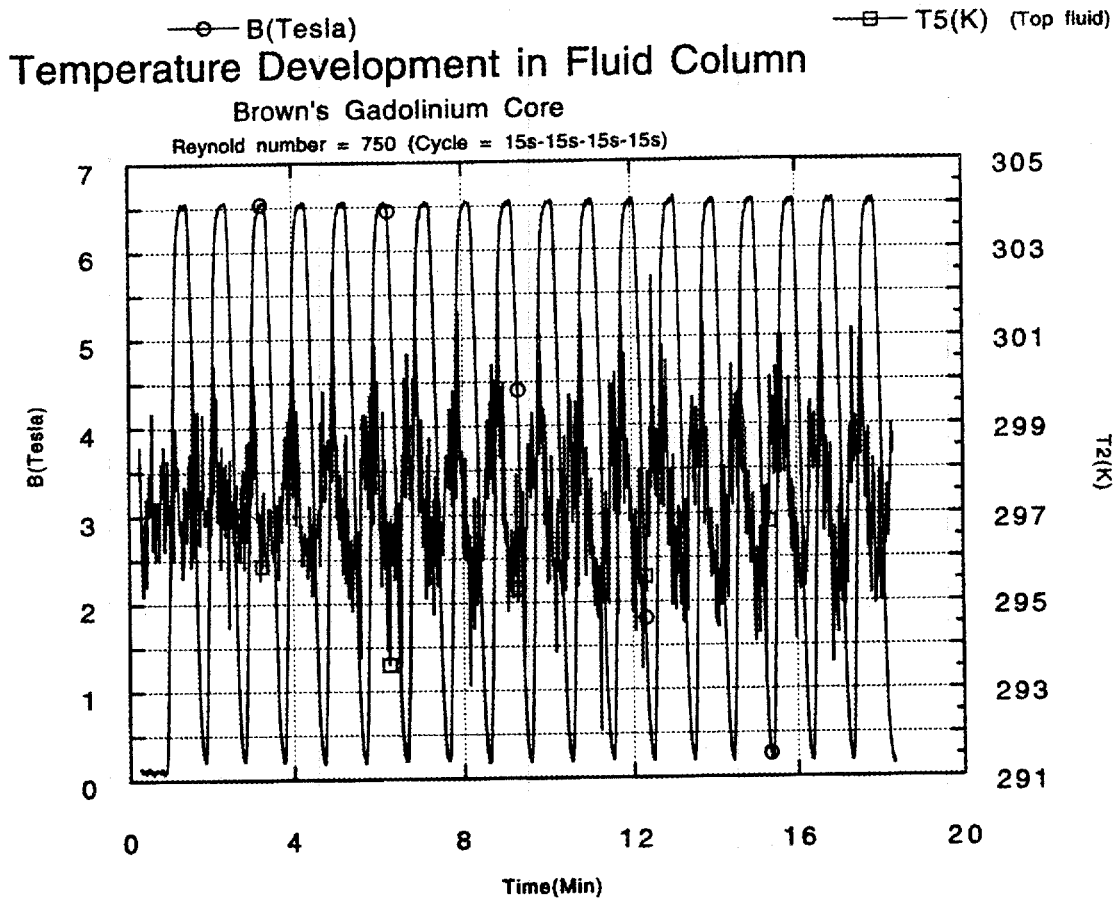


**Fig. B1.** Temperature development in the regenerator fluid column for the case of  $Re=750$  with 15s-15s of cycle period.

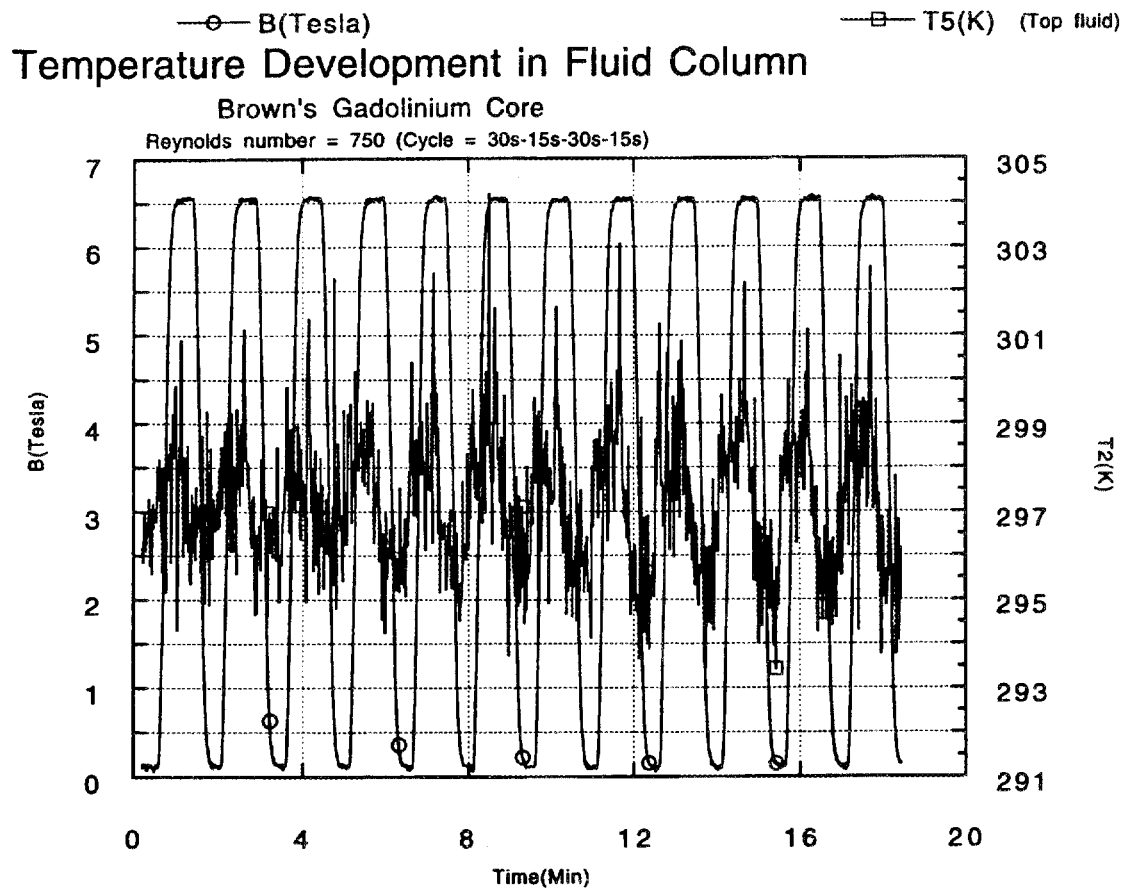


**Fig. B2. Temperature development in the regenerator fluid column for the case of  $Re=750$  with 30s-15s of cycle period.**

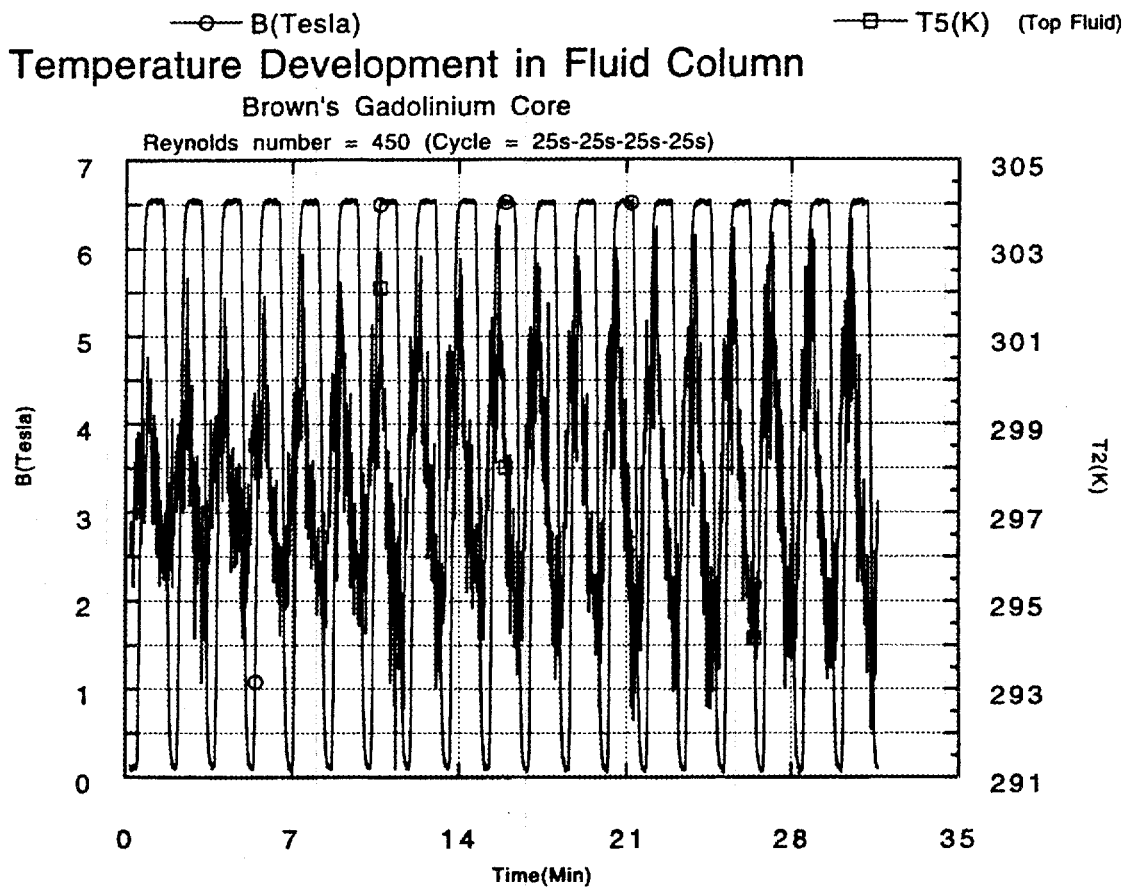


**Fig. B3. Temperature development in the regenerator fluid column for the case of  $Re=450$  with 25s-25s of cycle period.**

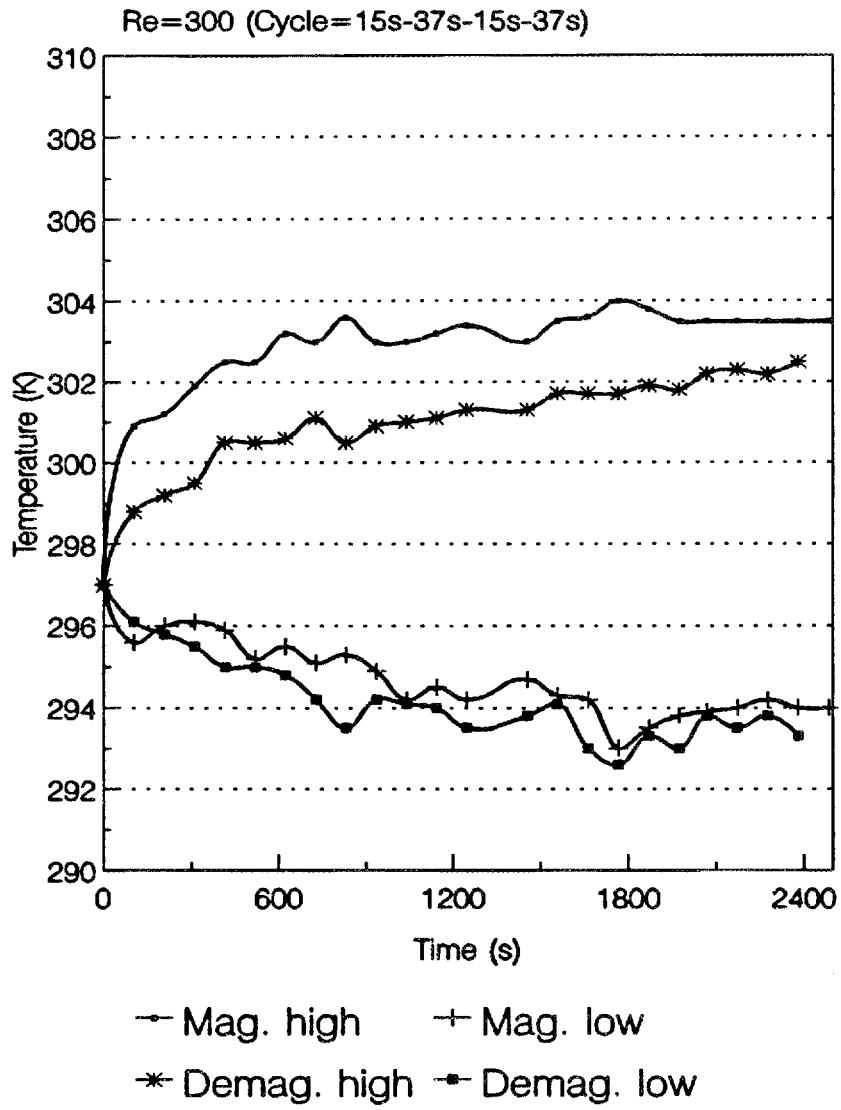


**Fig. B4.** Development of extreme temperatures in the regenerator fluid column for the case of Re=300 with 15s-37s of cycle period.

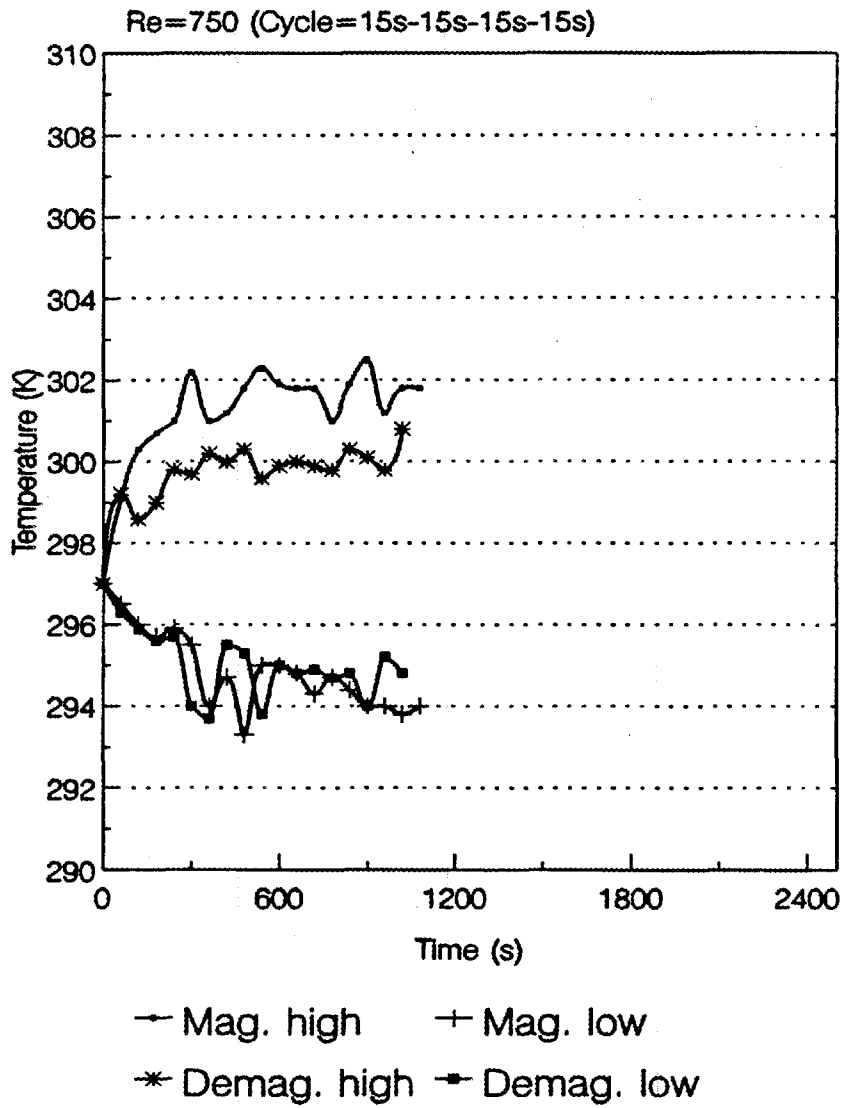


**Fig. B5. Development of extreme temperatures in the regenerator fluid column for the case of Re=750 with 15s-15s of cycle period.**

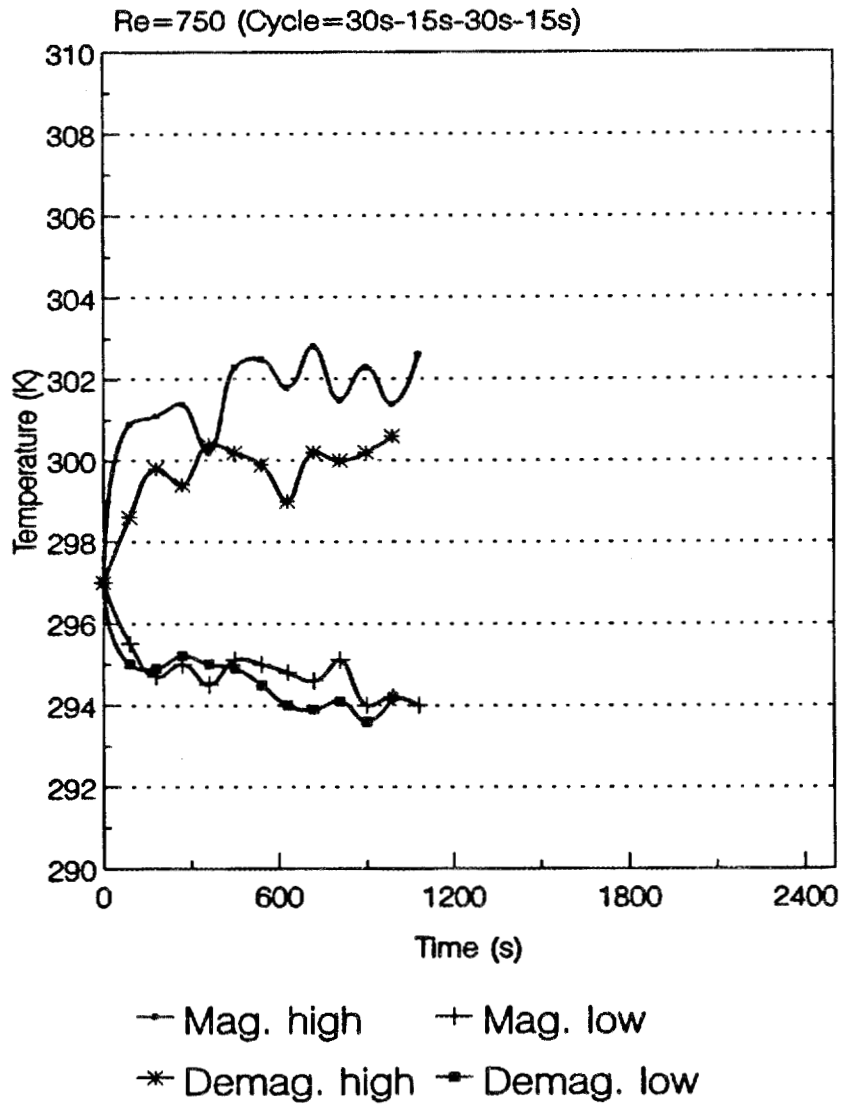


**Fig. B6. Development of extreme temperatures in the regenerator fluid column for the case of Re=750 with 30s-15s of cycle period.**

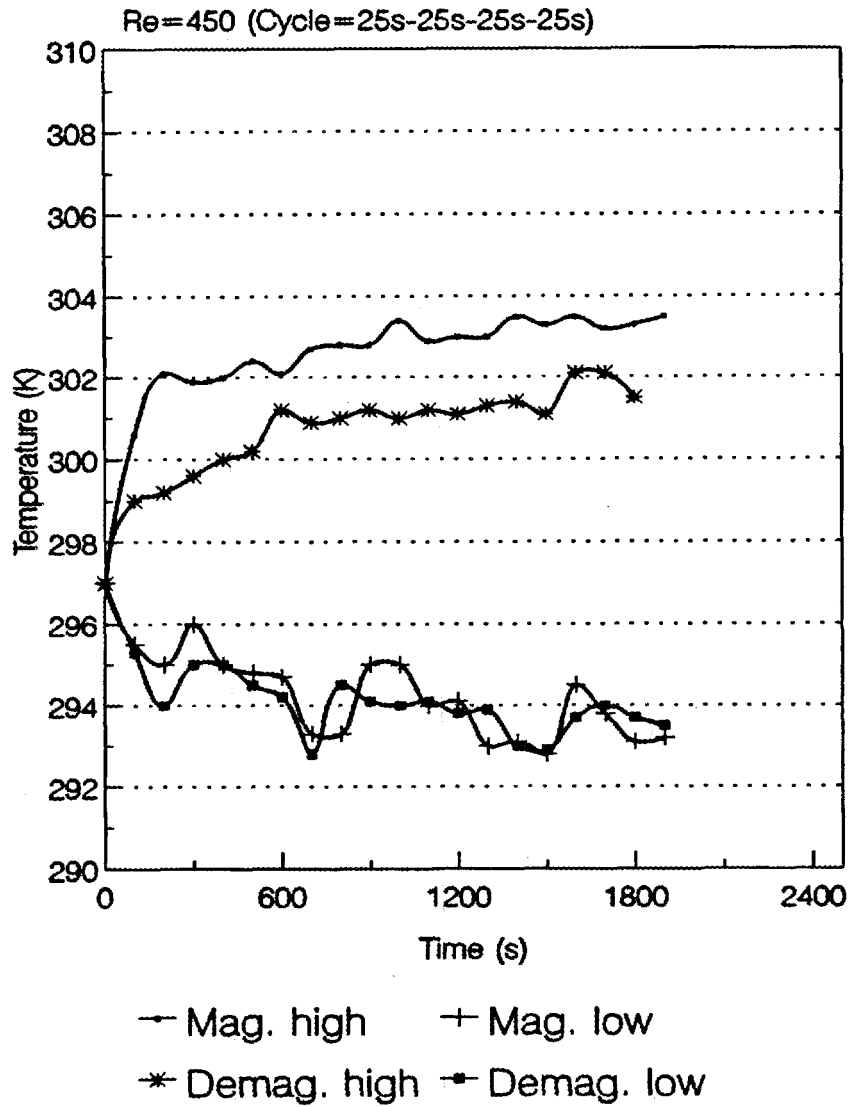


**Fig. B7. Development of extreme temperatures in the regenerator fluid column for the case of Re=450 with 25s-25s of cycle period.**



**INTERNAL DISTRIBUTION**

- |                     |                                |
|---------------------|--------------------------------|
| 1. R. S. Carlsmith  | 27. R. W. Murphy               |
| 2-8. D. T. Chen     | 28. W. Schwenterly             |
| 9-18. F. C. Chen    | 29. R. B. Shelton              |
| 19. G. L. Chen      | 30. T. Wilson                  |
| 20. D. M. Counce    | 31. P. P. Wolff                |
| 21. G. E. Courville | 32. ORNL Patent Office         |
| 22. W. Fulkerson    | 33. Central Research Library   |
| 23. M. A. Kuliasha  | 34. Document Reference Section |
| 24. M. S. Lubell    | 35-37. Laboratory Records      |
| 25. J. W. Lue       | 38. Laboratory Records - RC    |
| 26. V. C. Mei       |                                |

**EXTERNAL DISTRIBUTION**

39. D. R. Bohi, Director, Energy and Natural Resources Division, Resources for the Future, 1616 P Street, NW, Washington, DC 20036
40. T. E. Drabek, Department of Sociology, University of Denver, Denver, CO 80208-0209
41. E. P. HuangFu, Advanced Industrial Concepts Division, Department of Energy, EE-232, 5F-059/FORRESTAL, 1000 Independence Avenue, SW, Washington, DC 20585
42. R. O. Hultgren, Energy Research and Development, Department of Energy, Oak Ridge National Laboratory, P. O. Box 2008, Oak Ridge, TN 37831-6269
43. N. Lombardo, Pacific Northwest Laboratory, Battelle Boulevard, Richland, VA 99351
44. C. D. MacCracken, President, Calmac Manufacturing Corporation, 101 West Sheffield Avenue, P. O. Box 710, Englewood, NJ 07631
45. T. J. Marciniak, Argonne National Laboratory, ES-362-4AA, Building 362, 9700 South Cass Avenue, Argonne, IL 60439-4815
46. J. Scott, Science/Engineering Education Division, Oak Ridge Associated Universities, Oak Ridge, TN 37831
47. J. B. Shrago, Director, Office of Technology Transfer, 405 Kirkland Hall, Vanderbilt University, Nashville, TN 37240
48. M. S. Sohal, Idaho National Engineering Laboratory, EG&G Idaho, Inc., P. O. Box 1625, Idaho Falls, ID 83415
49. G. F. Sowers, P. E., Senior Vice President, Law Companies Group, Inc., 114 Townpark Drive, Suite 250, Kennesaw, GA 30144-5599
50. C. M. Walton, Ernest H. Cockrell Centennial Chair in Engineering and Chairman, Department of Civil Engineering, University of Texas at Austin, Austin, TX 78712-1076
- 51-52. Office of Scientific and Technical Information, P. O. Box 62, Oak Ridge, TN 37831